Soil Strength and Slope Stability

J. Michael Duncan
Stephen G. Wright

WILEY
JOHN WILEY & SONS, INC.

CONTENTS

	Preface	ix
CHAPTER 1	INTRODUCTION	1
CHAPTER 2	EXAMPLES AND CAUSES OF SLOPE FAILURE	5
	Examples of Slope Failure	5
	Causes of Slope Failure	14
	Summary	17
CHAPTER 3	SOIL MECHANICS PRINCIPLES	19
	Drained and Undrained Conditions	19
	Total and Effective Stresses	21
	Drained and Undrained Shear Strengths	22
	Basic Requirements for Slope Stability Analyses	26
CHAPTER 4	STABILITY CONDITIONS FOR ANALYSES	31
	End-of-Construction Stability	31
	Long-Term Stability	32
	Rapid (Sudden) Drawdown	32
	Earthquake	33
	Partial Consolidation and Staged Construction	33
	Other Loading Conditions	33
CHAPTER 5	SHEAR STRENGTHS OF SOIL AND MUNICIPAL SOLID WASTE	35
	Granular Materials	35
	Silts	40
	Clays	44
	Municipal Solid Waste	54
CHAPTER 6	MECHANICS OF LIMIT EQUILIBRIUM PROCEDURES	55
	Definition of the Factor of Safety	55
	Equilibrium Conditions	56
	Single Free-Body Procedures	57
	Procedures of Slices: General	63

Procedures of Slices: Circular Slip Surfaces 63
Procedures of Slices: Noncircular Slip Surfaces 71
Assumptions, Equilibrium Equations, and Unknowns 83
Representation of Interslice Forces (Side Forces) 83
Computations with Anisotropic Shear Strengths 90
Computations with Curved Failure Envelopes and Anisotropic Shear Strengths 90
Alternative Definitions of the Factor of Safety 91
Pore Water Pressure Representation 95

CHAPTER 7 METHODS OF ANALYZING SLOPE STABILITY 103

Simple Methods of Analysis 103
Slope Stability Charts 105
Spreadsheet Software 107
Computer Programs 107
Verification of Analyses 111
Examples for Verification of Stability Computations 112

CHAPTER 8 REINFORCED SLOPES AND EMBANKMENTS 137

Limit Equilibrium Analyses with Reinforcing Forces 137
Factors of Safety for Reinforcing Forces and Soil Strengths 137
Types of Reinforcement 139
Reinforcement Forces 139
Allowable Reinforcement Forces and Factors of Safety 141
Orientation of Reinforcement Forces 142
Reinforced Slopes on Firm Foundations 142
Embankments on Weak Foundations 145

CHAPTER 9 ANALYSES FOR RAPID DRAWDOWN 151

Drawdown during and at the End of Construction 151
Drawdown for Long-Term Conditions 151
Partial Drainage 160

CHAPTER 10 SEISMIC SLOPE STABILITY 161

Analysis Procedures 161
Pseudostatic Screening Analyses 164
Determining Peak Accelerations 165
Shear Strength for Pseudostatic Analyses 166
Postearthquake Stability Analyses 169

CHAPTER 11 ANALYSES OF EMBANKMENTS WITH PARTIAL CONSOLIDATION OF WEAK FOUNDATIONS 175

Consolidation during Construction 175
Analyses of Stability with Partial Consolidation 176

Observed Behavior of an Embankment Constructed in Stages 178
Discussion 179

CHAPTER 12 ANALYSES TO BACK-CALCULATE STRENGTHS 183

Back-Calculating Average Shear Strength 183
Back-Calculating Shear Strength Parameters Based on Slip Surface Geometry 185
Examples of Back-Analyses of Failed Slopes 187
Practical Problems and Limitation of Back-Analyses 195
Other Uncertainties 197

CHAPTER 13 FACTORS OF SAFETY AND RELIABILITY 199

Definitions of Factor of Safety 199
Factor of Safety Criteria 200
Reliability and Probability of Failure 200
Standard Deviations and Coefficients of Variation 202
Coefficient of Variation of Factor of Safety 205
Reliability Index 206
Probability of Failure 206

CHAPTER 14 IMPORTANT DETAILS OF STABILITY ANALYSES 213

Location of Critical Slip Surfaces 213
Examination of Noncritical Shear Surfaces 219
Tension in the Active Zone 221
Inappropriate Forces in the Passive Zone 224
Other Details 228
Verification of Calculations 232
Three-Dimensional Effects 233

CHAPTER 15 PRESENTING RESULTS OF STABILITY EVALUATIONS 237

Site Characterization and Representation 237
Soil Property Evaluation 238
Pore Water Pressures 238
Special Features 238
Calculation Procedure 239
Analysis Summary Figure 239
Parametric Studies 241
Detailed Input Data 243
Table of Contents 243

CHAPTER 16 SLOPE STABILIZATION AND REPAIR 247

Use of Back-Analysis 247
Factors Governing Selection of Method of Stabilization 247

	Drainage	248
	Excavations and Buttress Fills	253
	Retaining Structures	254
	Reinforcing Piles and Drilled Shafts	256
	Injection Methods	260
	Vegetation	261
	Thermal Treatment	261
	Bridging	262
	Removal and Replacement of the Sliding Mass	263
APPENDIX	SLOPE STABILITY CHARTS	265
	Use and Applicability of Charts for Analysis of Slope Stability	265
	Averaging Slope Inclinations, Unit Weights, and Shear Strengths	265
	Soils with $\phi = 0$	266
	Soils with $\phi > 0$	270
	Infinite Slope Charts	272
	Soils with $\phi = 0$ and Strength Increasing with Depth	274
	Examples	274
	References	281
	Index	295

surface and (2) the shear stress required for equilibrium.

The *factor of safety* for the shear surface is the ratio of the shear strength of the soil divided by the shear stress required for equilibrium. The normal stresses along the slip surface are needed to evaluate the shear strength: Except for soils with $\phi = 0$, the shear strength depends on the normal stress on the potential plane of failure.

In effective stress analyses, the pore pressures along the shear surface are subtracted from the total stresses to determine effective normal stresses, which are used to evaluate shear strengths. Therefore, to perform effective stress analyses, it is necessary to know (or to estimate) the pore pressures at every point along the shear surface. These pore pressures can be evaluated with relatively good accuracy for drained conditions, where their values are determined by hydrostatic or steady seepage boundary conditions. Pore pressures can seldom be evaluated accurately for undrained condtions, where their values are determined by the response of the soil to external loads.

In total stress analyses, pore pressures are not subtracted from the total stresses, because shear strengths are related to total stresses. Therefore, it is not necessary to evaluate and subtract pore pressures to perform total stress analyses. Total stress analyses are applicable only to undrained conditions. The basic premise of *total stress analysis* is this: The pore pressures due to undrained loading are determined by the behavior of the soil. For a given value of total stress on the potential failure plane, there is a unique value of pore pressure and therefore a unique value of effective stress. Thus, although it is true that shear strength is really controlled by effective stress, it is possible for the undrained condition to relate shear strength to total normal stress, because effective stress and total stress are uniquely related for the undrained condition. Clearly, this line of reasoning does not apply to drained conditions, where pore pressures are controlled by hydraulic boundary conditions rather than the response of the soil to external loads.

Analyses of Drained Conditions

Drained conditions are those where changes in load are slow enough, or where they have been in place long enough, so that all of the soils reach a state of equilibrium and no excess pore pressures are caused by the loads. In drained conditions pore pressures are controlled by hydraulic boundary conditions. The water within the soil may be static, or it may be seeping steadily, with no change in the seepage over time and no increase or decrease in the amount of water within the soil. If these conditions prevail in all the soils at a site, or if the conditions at a site can reasonably be approximated by these conditions, a drained analysis is appropriate. A *drained analysis* is performed using:

- Total unit weights
- Effective stress shear strength parameters
- Pore pressures determined from hydrostatic water levels or steady seepage analyses

Analyses of Undrained Conditions

Undrained conditions are those where changes in loads occur more rapidly than water can flow in or out of the soil. The pore pressures are controlled by the behavior of the soil in response to changes in external loads. If these conditions prevail in the soils at a site, or if the conditions at a site can reasonably be approximated by these conditions, an undrained analysis is appropriate. An *undrained analysis* is performed using:

- Total unit weights
- Total stress shear strength parameters

How Long Does Drainage Take?

As discussed earlier, the difference between undrained and drained conditions is time. The drainage characteristics of the soil mass, and its size, determine how long will be required for transition from an undrained to a drained condition. As shown by Eq. (3.1):

$$t_{99} = 4\frac{D^2}{c_v} \tag{3.17}$$

where t_{99} is the time required to reach 99% of drainage equilibrium, D the length of the drainage path, and c_v the coefficient of consolidation.

Values of c_v for clays vary from about 1.0 cm^2/h (10 ft^2/yr) to about 100 times this value. Values of c_v for silts are on the order of 100 times the values for clays, and values of c_v for sands are on the order of 100 times the values for silts, and higher. These typical values can be used to develop some rough ideas of the lengths of time required to achieve drained conditions in soils in the field.

Drainage path lengths are related to layer thicknesses. They are half the layer thickness for layers that are bounded on both sides by more permeable soils, and they are equal to the layer thickness for layers that are drained only on one side. Lenses or layers of silt or sand within clay layers provide internal drainage, reducing the drainage path length to half of the thickness between internal drainage layers.

CHAPTER 5

Shear Strengths of Soil and Municipal Solid Waste

A key step in analyses of soil slope stability is measuring or estimating the strengths of the soils. Meaningful analyses can be performed only if the shear strengths used are appropriate for the soils and for the particular conditions analyzed. Much has been learned about the shear strength of soils within the past 60 years, often from surprising and unpleasant experience with the stability of slopes, and many useful research studies of soil strength have been performed. The amount of information that has been amassed on soil strengths is very large. The following discussion focuses on the principles that govern soil strength, the issues that are of the greatest general importance in evaluating strength, and strength correlations that have been found useful in practice. The purpose is to provide information that will establish a useful framework and a point of beginning for detailed studies of the shear strengths of soils at particular sites.

GRANULAR MATERIALS

The strength characteristics of all types of granular materials (sands, gravels, and rockfills) are similar in many respects. Because the permeabilities of these materials are high, they are usually fully drained in the field, as discussed in Chapter 3. They are cohesionless: The particles do not adhere to one another, and their effective stress shear strength envelopes pass through the origin of the Mohr stress diagram.

The shear strength of these materials can be characterized by the equation

$$s = \sigma' \tan \phi' \tag{5.1}$$

where s is the shear strength, σ' the effective normal stress on the failure plane, and ϕ' the effective stress angle of internal friction. Measuring or estimating the drained strengths of these materials involves determining or estimating appropriate values of ϕ'.

The most important factors governing values of ϕ' for granular soils are density, confining pressure, grain-size distribution, strain boundary conditions, and the factors that control the amount of particle breakage during shear, such as the types of mineral and the sizes and shapes of particles.

Curvature of Strength Envelope

Mohr's circles of stress at failure for four triaxial tests on the Oroville Dam shell material are shown in Figure 5.1. Because this material is cohesionless, the Mohr–Coulomb strength envelope passes through the origin of stresses, and the relationship between strength and effective stress on the failure plane can be expressed by Eq. (5.1).

A *secant value* of ϕ' can be determined for each of the four triaxial tests. This value corresponds to a linear failure envelope going through the origin and passing tangent to the circle of stress at failure for the particular test, as shown in Figure 5.1. The dashed line in Figure 5.1 is the linear strength envelope for the test with the highest confining pressure. The secant value of ϕ' for an individual test is calculated as

$$\phi' = 2\left[\left(\tan^{-1}\sqrt{\frac{\sigma'_{1f}}{\sigma'_{3f}}}\right) - 45^\circ\right] \tag{5.2}$$

where σ'_{1f} and σ'_{3f} are the major and minor principal stresses at failure. Secant values of ϕ' for the tests on Oroville Dam shell material shown in Figure 5.1 are given in Table 5.1, and the envelope for $\sigma'_3 = 4480$ kPa is shown in Figure 5.1.

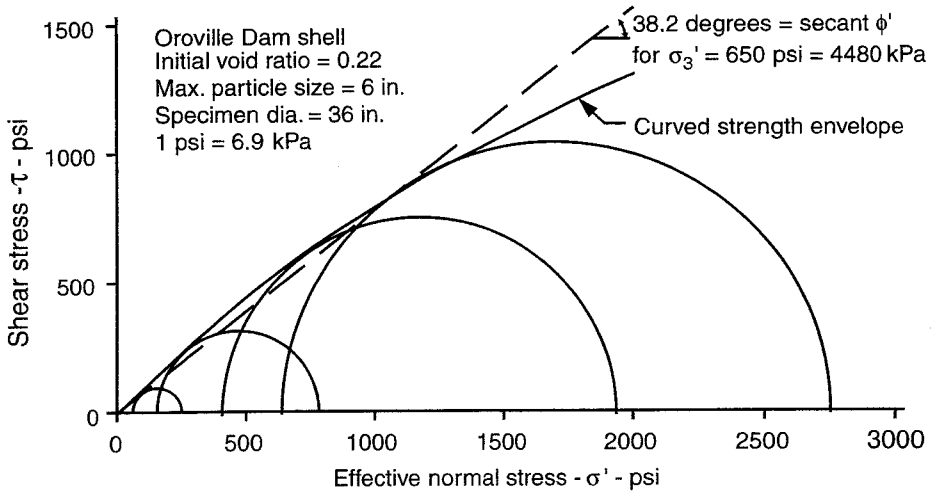

Figure 5.1 Mohr's circles of shear stress at failure and failure envelope for triaxial tests on Oroville Dam shell material. (Data from Marachi et al., 1969.)

Table 5.1 Stresses at Failure and Secant Values of ϕ' for Oroville Dam Shell Material

Test	σ_3' (kPa)	σ_1' (kPa)	ϕ' (deg)
1	210	1,330	46.8
2	970	5,200	43.4
3	2,900	13,200	39.8
4	4,480	19,100	38.2

The curvature of the envelope and the decrease in the secant value of ϕ' as the confining pressure increases are due to increased particle breakage as the confining pressure increases. At higher pressures the interparticle contact forces are larger. The greater these forces, the more likely it is that particles will be broken during shear rather than remaining intact and sliding or rolling over neighboring particles as the material is loaded. When particles break instead of rolling or sliding, it is because breaking requires less energy, and because the mechanism of deformation is changing as the pressures increase, the shearing resistance does not increase in exact proportion to the confining pressure. Even though the Oroville Dam shell material consists of hard amphibolite particles, there is significant particle breakage at higher pressures.

As a result of particle breakage effects, strength envelopes for all granular materials are curved. The envelope does pass through the origin, but the secant value of ϕ' decreases as confining pressure increases. Secant values of ϕ' for soils with curved envelopes can be characterized using two parameters, ϕ_0 and $\Delta\phi$:

$$\phi' = \phi_0 - \Delta\phi \log_{10} \frac{\sigma_3'}{p_a} \tag{5.3}$$

where ϕ' is the secant effective stress angle of internal friction, ϕ_0 the value of ϕ' for $\sigma_3' = 1$ atm, $\Delta\phi$ the reduction in ϕ' for a 10-fold increase in confining pressure, σ_3' the confining pressure, and p_a = atmospheric pressure. This relationship between ϕ' and σ_3' is shown in Figure 5.2*a*. The variation of ϕ' with σ_3' for the Oroville Dam shell material is shown in Figure 5.2*b*.

Values of ϕ' should be selected considering the confining pressures involved in the conditions being analyzed. Some slope stability computer programs have provisions for using curved failure envelopes, which is an effective means of representing variations of ϕ' with confining pressure. Alternatively, different values of ϕ' can be used for the same material, with higher values of ϕ' in areas where pressures are low and lower values of ϕ' in areas where pressures are high. In many cases, sufficient accuracy can be achieved by using a single value of ϕ' based on the average confining pressure.

Effect of Density

Density has an important effect on the strengths of granular materials. Values of ϕ' increase with density. For some materials the value of ϕ_0 increases by 15° or more as the density varies from the loosest to the densest state. Values of $\Delta\phi$ also increase with density, varying from zero for very loose materials to 10° or more for the same materials in a very dense state. An example is shown in Figure 5.3 for Sacramento River sand, a uniform fine sand composed predominantly of

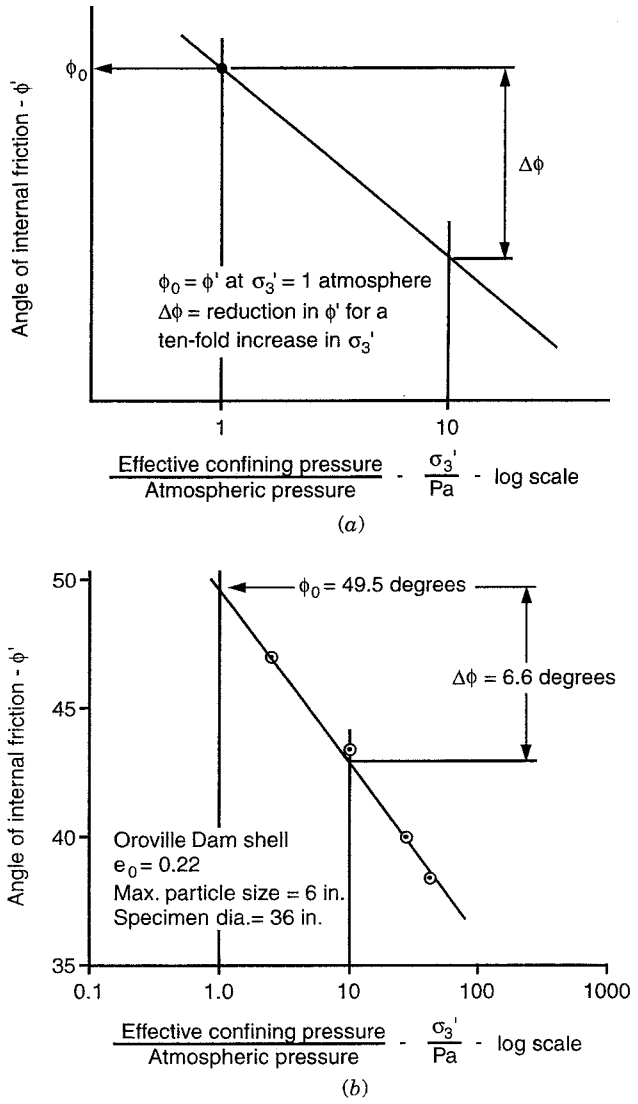

Figure 5.2 Effect of confining pressure on ϕ': (*a*) relationship between ϕ' and σ_3'; (*b*) variation of ϕ' and σ_3' for Oroville Dam shell.

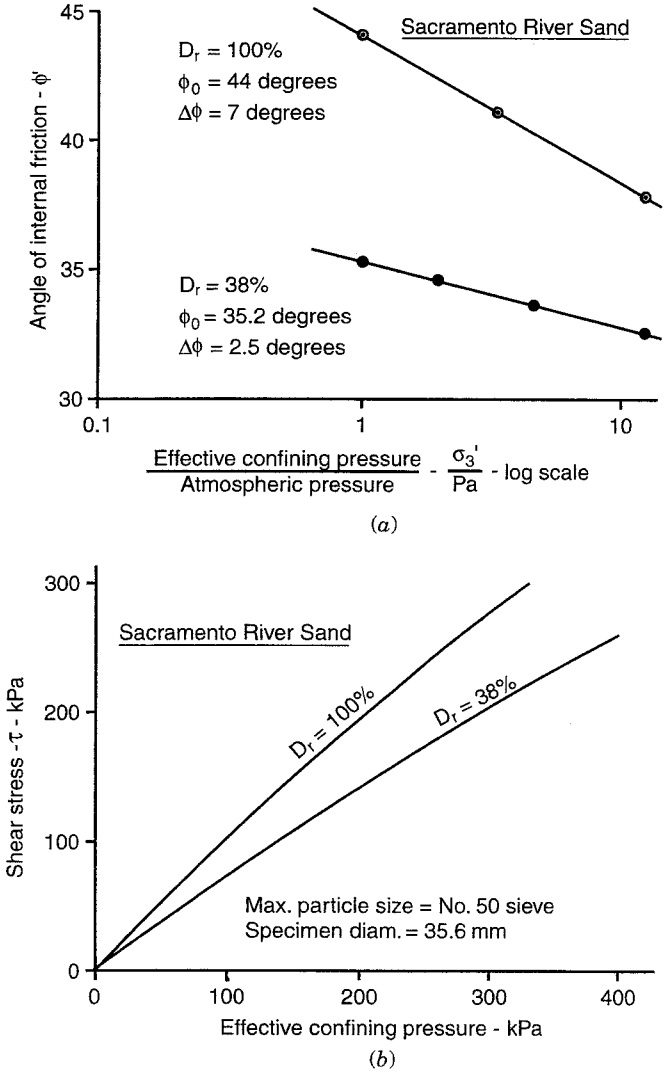

Figure 5.3 Effect of density on strength of Sacramento River sand: (*a*) variations of ϕ' with confining pressure; (*b*) strength envelopes. (Data from Lee and Seed, 1967.)

feldspar and quartz particles. At a confining pressure of 1 atm, ϕ_0 increases from 35° for D_r = 38% to 44° for D_r = 100%. The value of $\Delta\phi$ increases from 2.5° for D_r = 38% to 7° for D_r = 100%

Effect of Gradation

All other things being equal, values of ϕ' are higher for well-graded granular soils such as the Oroville Dam shell material (Figures 5.1 and 5.2) than for uniformly graded soils such as Sacramento River sand (Figure 5.3). In well-graded soils, smaller particles fill gaps between larger particles, and as a result it is possible to form a denser packing that offers greater resistance to shear. Well-graded materials are subject to segregation of particle sizes during fill placement and may form fills that are stratified, with alternating coarser and finer layers unless care is taken to ensure that segregation does not occur.

Plane Strain Effects

Most laboratory strength tests are performed using triaxial equipment, where a circular cylindrical test specimen is loaded axially and deforms with radial symmetry. In contrast, the deformations for many field conditions are close to plane strain. In plane strain, all displacements are parallel to one plane. In the field, this is usually the vertical plane. Strains and displace-

ments perpendicular to this plane are zero. For example, in a long embankment, symmetry requires that all displacements are in vertical planes perpendicular to the longitudinal axis of the embankment.

The value of ϕ' for plane strain conditions (ϕ'_{ps}) is higher than the value for triaxial conditions (ϕ'_t). Becker et al. (1972) found that the value of ϕ'_{ps} was 1 to 6° larger than the value of ϕ'_t for the same material at the same density, tested at the same confining pressure. The difference was greatest for dense materials tested at low pressures. For confining pressures below 100 psi (690 kPa), they found that ϕ'_{ps} was 3 to 6° larger than ϕ'_t.

Although there may be a significant difference between values of ϕ' measured in triaxial tests and the values most appropriate for conditions close to plane strain, this difference is usually ignored. It is conservative to ignore the difference and use triaxial values of ϕ' for plane strain conditions. This conventional practice provides an intrinsic additional safety margin for situations where the strain boundary conditions are close to plane strain.

Strengths of Compacted Granular Materials

When cohesionless materials are used to construct fills, it is normal to specify the method of compaction or

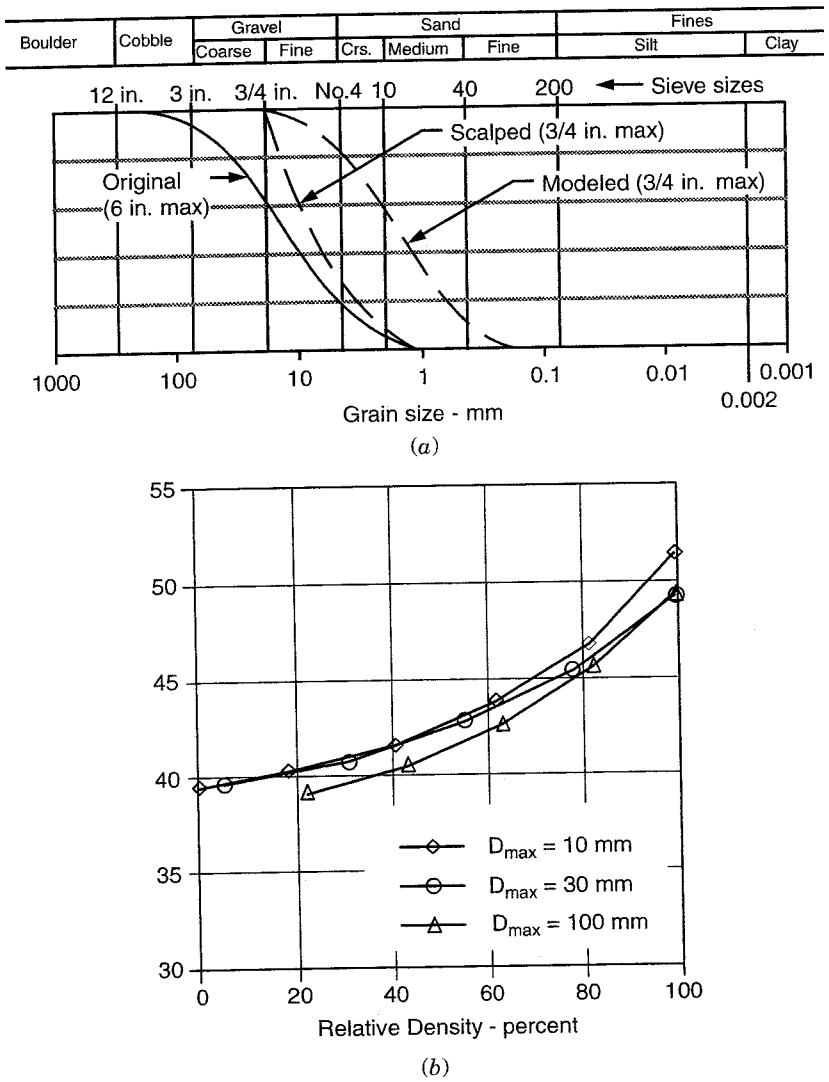

Figure 5.4 Modeling and scalping grain size curves and friction angles for scalped material: (*a*) grain-size curves for original, modeled, and scalped cobbely sandy gravel; (*b*) friction angles for scalped specimens of Goschenalp Dam rockfill. (After Zeller and Wullimann, 1957.)

the minimum acceptable density. Angles of internal friction for sands, gravels, and rockfills are strongly affected by density, and controlling the density of a fill is thus an effective way of ensuring that the fill will have the desired strength.

Minimum test specimen size. For the design of major structures such as dams, triaxial tests performed on specimens compacted to the anticipated field density are frequently used to determine values of ϕ'. The diameter of the triaxial test specimens should be at least six times the size of the largest soil particle, which can present problems for testing materials that contain large particles. The largest triaxial test equipment available in most soil mechanics laboratories is 100 to 300 mm (4 to 12 in.) in diameter. The largest particle sizes that can be tested with this equipment are thus about 16 to 50 mm (0.67 to 2 in.).

Modeling grain size curves and scalping. When soils with particles larger than one-sixth the triaxial specimen diameter are tested, particles that are too large must be removed. Becker et al. (1972) prepared test specimens with *modeled* grain-size curves. The curves for the modeled materials were parallel to the curve for the original material, as shown in Figure 5.4*a*. It was found that the strengths of the model materials were essentially the same as the strengths of the original materials, provided that the test specimens were prepared at the same relative density, D_r:

$$D_r = \frac{e_{\max} - e}{e_{\max} - e_{\min}} \times 100\% \qquad (5.4)$$

where D_r is the relative density, $e_{\max}$ the maximum void ratio, e the void ratio, and $e_{\min}$ the minimum void ratio.

Becker et al. (1972) found that removing large particles changed the maximum and minimum void ratios of the material, and as a result, *the same relative density was not the same void ratio for the original and model materials.* The grain-size modeling technique used by Becker et al. (1972) can be difficult to use for practical purposes. When a significant quantity of coarse material has to be removed, there may not be enough fine material available to develop the model grain-size curve. An easier technique is *scalping,* where the large sizes are not replaced with smaller sizes. A scalped gradation is shown in Figure 5.4*a*.

The data in Figure 5.4*b* show that the value of ϕ' for scalped test specimens is essentially the same as for the original material, *provided that all specimens are prepared at the same relative density.* Again, *the same relative density will not be the same void ratio for the original and scalped materials.*

Controlling field densities. Using relative density to control the densities of laboratory test specimens does not imply that it is necessary to use relative density for control of density in the field during construction. Controlling the density of granular fills in the field using relative density has been found to be difficult, especially when the fill material contains large particles. Specifications based on method of compaction, or on relative compaction, can be used for field control, even though relative density may be used in connection with laboratory tests.

Strengths of Natural Deposits of Granular Materials

It is not possible to obtain undisturbed samples of granular materials, except by exotic procedures such as freezing and coring the ground. In most cases friction angles for natural deposits of granular materials are estimated using the results of in situ tests such as the standard penetration test (SPT) or the cone penetration test (CPT). Correlations that can be used to interpret values of ϕ' from in situ tests are discussed below.

Strength correlations. Many useful correlations have been developed that can be used to estimate the strengths of sands and gravels based on correlations with relative densities or the results of in situ tests. The earliest correlations were developed before the influence of confining pressure on ϕ' was well understood. More recent correlations take confining pressure into account by correlating both ϕ_0 and $\Delta\phi$ with relative density or by including overburden pressure in correlations between ϕ' and the results of in situ tests.

Table 5.2 relates values of ϕ_0 and $\Delta\phi$ to relative density values for well-graded sands and gravels, poorly graded sands and gravels, and silty sands. Figures 5.5 and 5.6 can be used to estimate in situ relative density based on SPT blow count or CPT cone resistance. Values of relative density estimated using Figure 5.5 or 5.6 can be used together with Table 5.2 to estimate values of ϕ_0 and $\Delta\phi$ for natural deposits.

Figures 5.7 and 5.8 relate values of ϕ' to overburden pressure and SPT blow count or CPT cone resistance. Figure 5.9 relates ϕ' to relative density for sands. The values of ϕ' in Figure 5.9 correspond to confining pressures of about 1 atm, and are close to the values of ϕ_0 listed in Table 5.2. Tables 5.3 and 5.4 relate values of ϕ' to SPT blow count and CPT cone resistance. The correlations are easy to use, but they do not take the effect of confining pressure into account.

Recapitulation

- The drained shear strengths of sands, gravels, and rockfill materials can be expressed as $s = \sigma' \tan \phi'$.
- Values of ϕ' for these materials are controlled by density, gradation, and confining pressure.
- The variation of ϕ' with confining pressure can be represented by

$$\phi' = \phi_0 - \Delta\phi \log_{10} \frac{\sigma_3'}{p_a}$$

  where σ_3' is the confining pressure and p_a is atmospheric pressure.
- When large particles are removed to prepare specimens for laboratory tests, the test specimens should be prepared at the same relative density as the original material, not the same void ratio.
- Values of ϕ' for granular materials can be estimated based on the Unified Soil Classification, relative density, and confining pressure.
- Values of ϕ' for granular materials can also be estimated based on results of standard penetration tests or cone penetration tests.

Table 5.2 Values of ϕ_0 and $\Delta\phi$ for Sands and Gravels

Unified classification	Standard Proctor RC[a] (%)	Relative density, D_r[b] (%)	ϕ_0[c] (deg)	$\Delta\phi$ (deg)
GW, SW	105	100	46	10
	100	75	43	8
	95	50	40	6
	90	25	37	4
GP, SP	105	100	42	9
	100	75	39	7
	95	50	36	5
	90	25	33	3
SM	100	—	36	8
	95	—	34	6
	90	—	32	4
	85	—	30	2

Source: Wong and Duncan (1974).

[a]RC = relative compaction = $\gamma_d/\gamma_{d\,\max} \times 100\%$.

[b]$D_r = (e_{\max} - e)/e_{\max} - e_{\min}) \times 100\%$.

[c]$\phi' = \phi_0 - \Delta\phi \log_{10} \sigma_3'/p_a$ where p_a is atmospheric pressure.

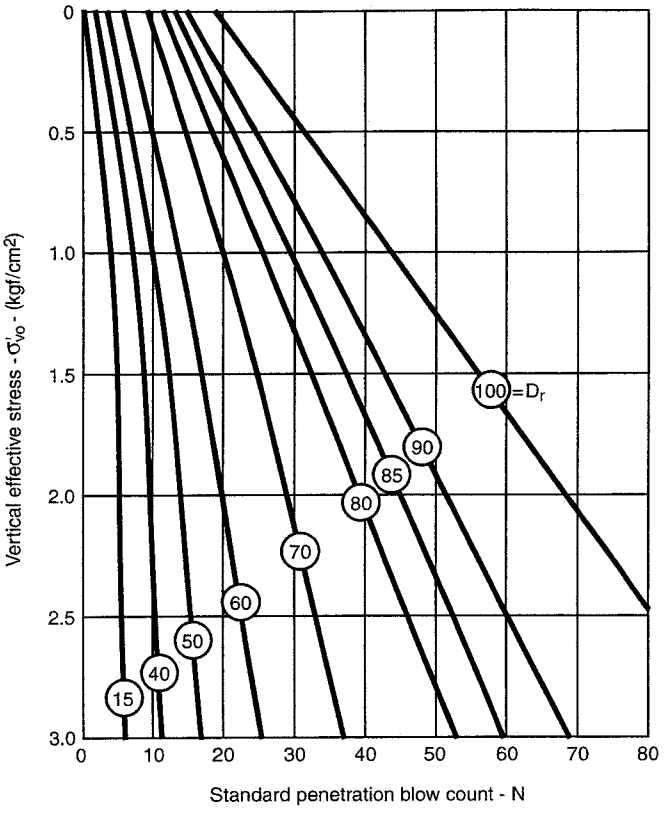

Figure 5.5 Relationship among SPT blow count, overburden pressure, and relative density for sands. (After Gibbs and Holtz, 1957, and U.S. Dept. Interior, 1974.)

SILTS

The shear strength of silts in terms of effective stress can be expressed by the Mohr–Coulomb strength criterion as

$$s = c' + \sigma' \tan \phi' \tag{5.5}$$

where s is the shear strength, c' the effective stress cohesion intercept, and ϕ' the effective stress angle of internal friction.

The behavior of silts has not been studied as extensively and is not as well understood as the behavior of granular materials or clays. Although the strengths of silts are governed by the same principles as the strengths of other soils, the range of their behavior is wide, and sufficient data are not available to anticipate or estimate their properties with the same degree of reliability as is possible in the case of granular soils or clays.

Silts encompass a broad range of behavior, from behavior that is very similar to the behavior of fine sands

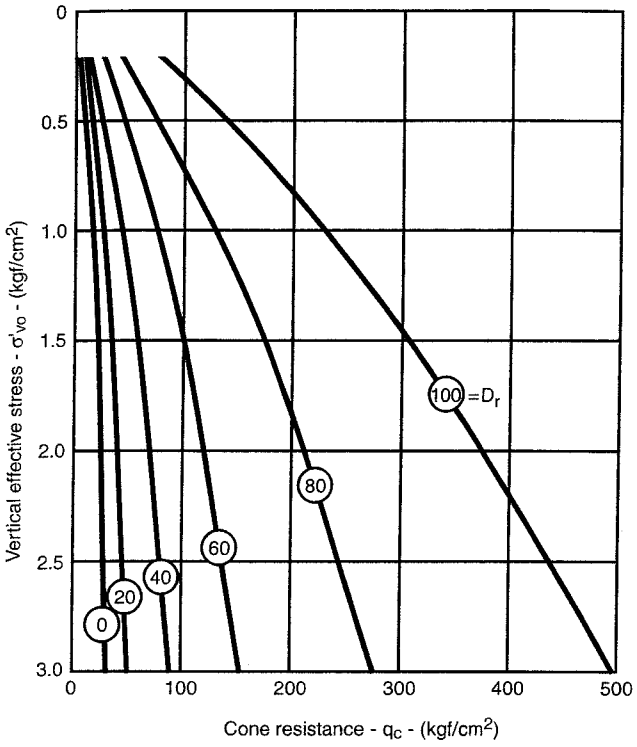

Figure 5.6 Relationship among CPT cone resistance, overburden pressure, and relative density of sands. (After Schmertmann, 1975.)

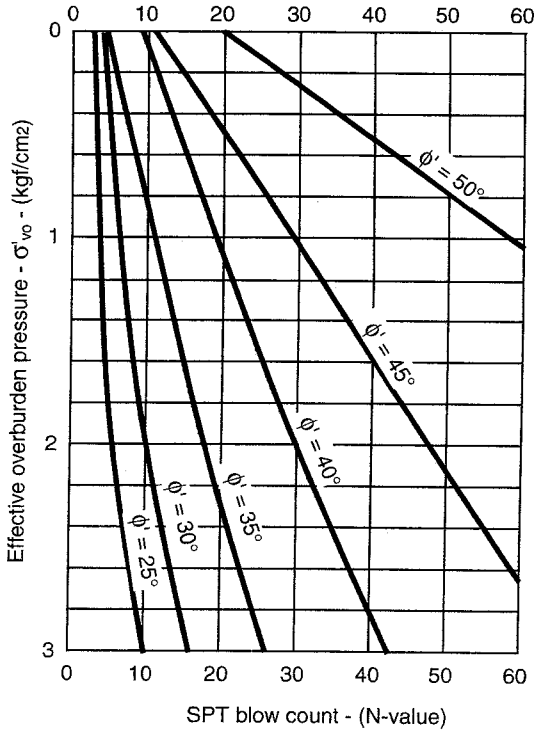

Figure 5.7 Relationship among SPT blow count, overburden pressure, and ϕ' for sands. (After DeMello, 1971, and Schmertmann, 1975.)

at one extreme to behavior that is essentially the same as the behavior of clays at the other extreme. It is useful to consider silts in two distinct categories: nonplastic silts, which behave more like fine sands, and plastic silts, which behave more like clays.

Nonplastic silts, like the silt of which Otter Brook Dam was constructed, behave similarly to fine sands. Nonplastic silts, however, have some unique characteristics, such as lower permeability, that influence their behavior and deserve special consideration.

An example of highly plastic silt is San Francisco Bay mud, which has a liquid limit near 90, a plasiticity index near 45, and classifies as MH (a silt of high plasticity) by the Unified Soil Classification System. San Francisco Bay mud behaves like a normally consolidated clay. The strength characteristics of clays discussed later in this chapter are applicable to materials such as San Francisco Bay mud.

Sample Disturbance

Disturbance during sampling is a serious problem in nonplastic silts. Although they are not highly sensitive by the conventional measure of sensitivity (sensitivity

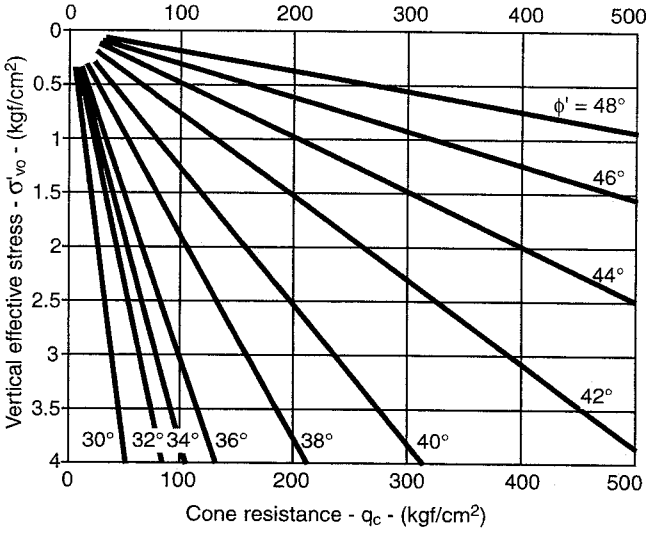

Figure 5.8 Relationship between CPT cone resistance, overburden pressure, and ϕ' for sands. (After Robertson and Campanella, 1983.)

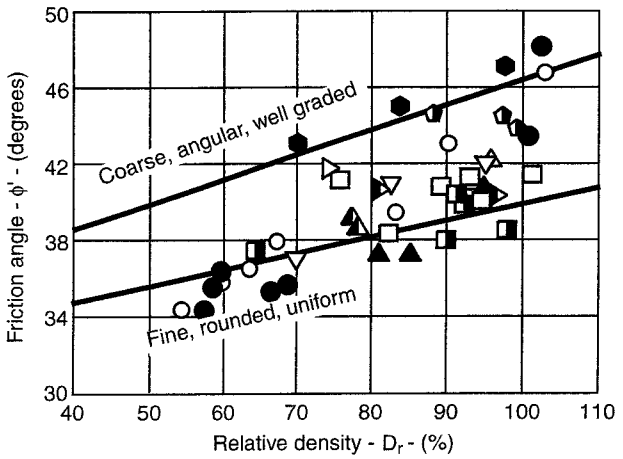

Figure 5.9 Correlation between friction angle and relative density for sands. (Data from Schmertmann, 1975, and Lunne and Kleven, 1982.)

Table 5.3 Relationship Among Relative Density, SPT Blow Count, and Angle of Internal Friction for Clean Sands

State of packing	Relative density, D_r (%)	SPT blow count, N^a (blows/ft)	Angle of internal friction ϕ'^b (deg)
Very loose	< 20	< 4	< 30
Loose	20–40	4–10	30–35
Compact	40–60	10–30	35–40
Dense	60–80	30–50	40–45
Very dense	> 80	> 50	> 45

Source: Meyerhof (1956).

[a] $N = 15 + (N' - 15)/2$ for $N' > 15$ in saturated very fine or silty sand, where N is the blow count corrected for dynamic pore pressure effects during the SPT, and N' is the measured blow count.

[b] Reduce ϕ' by 5° for clayey sand; increase ϕ' by 5° for gravelly sand.

= undisturbed strength/remoulded strength), they are very easily disturbed. In a study of a silt from the Alaskan arctic (Fleming and Duncan, 1990), it was found that disturbance reduced the undrained strengths measured in unconsolidated–undrained tests by as much as 40%, and increased the undrained strengths measured in consolidated–undrained tests by as much as 40%. Although silts can usually be sampled using the same techniques as those used for clays, the quality of samples should not be expected to be as good.

Table 5.4 Correlation Among Relative Density, CPT Cone Resistance, and Angle of Internal Friction for Clean Sands

State of packing	Relative density, D_r (%)	q_c (tons/ft² or kgf/cm²)	ϕ' (deg)
Very loose	< 20	< 20	< 32
Loose	20–40	20–50	32–35
Medium	40–60	50–150	35–38
Dense	60–80	150–250	38–41
Very dense	> 80	250–400	41–45

Source: Meyerhof (1976).

Cavitation

Unlike clays, nonplastic silts almost always tend to dilate when sheared, even if they are normally consolidated. In undrained tests, pore pressures decrease as a result of this tendency to dilate, and pore pressures can become negative. When pore pressures are negative, dissolved air or gas may come out of solution, forming bubbles within test specimens that greatly affect their behavior.

Figure 5.10 shows stress–strain and pore pressure–strain curves for consolidated–undrained triaxial tests on nonplastic silt from the Yazoo River valley. As the specimens were loaded, they tended to dilate, and the pore pressures decreased. As the pore pressures decreased, the effective confining pressures increased. The effective stresses stopped increasing when cavitation occurred, because from that point on the volume of the specimens increased as the cavitation bubbles expanded. The value of the maximum deviator stress for each sample was determined by the initial pore pressure (the back pressure), which determined how much negative change in pore pressure took place before cavitation occurred. The higher the back pressure, the greater was the undrained strength. These effects can be noted in Figure 5.10.

Drained or Undrained Strength?

Values of c_v for nonplastic silts are often in the range 100 to 10,000 cm²/h (1000 to 100,000 ft²/yr). It is often difficult to determine whether silts will be drained or undrained under field loading conditions,

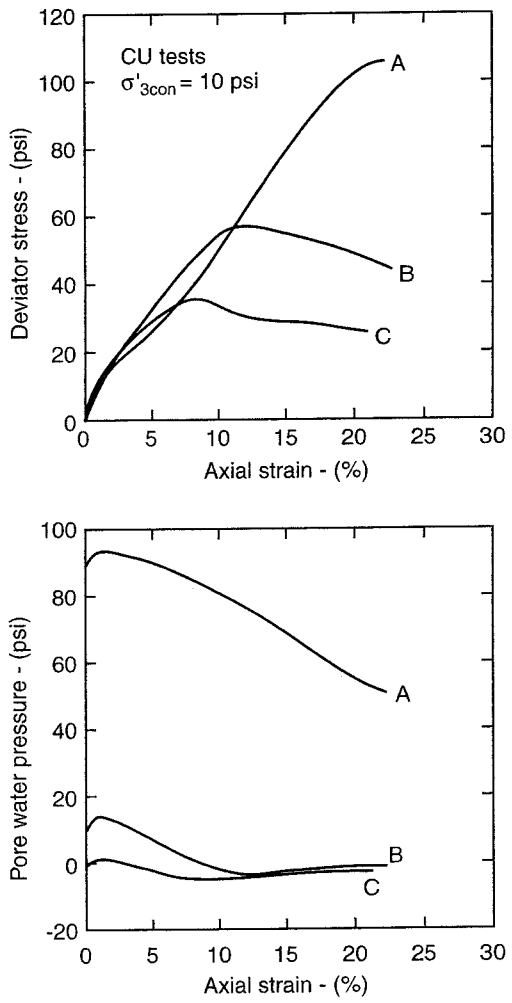

Figure 5.10 Effect of cavitation on undrained strength of reconstituted Yazoo silt. (From Rose, 1994.)

and in many cases it is prudent to consider both possibilities.

Strengths of Compacted Silts

Laboratory test programs for silts to be used as fills can be conducted following the principles that have been established for testing clays. Silts are moisture-sensitive and compaction characteristics are similar to those for clays. Densities can be controlled effectively using relative compaction. Undrained strengths of both plastic and nonplastic silts at the as-compacted condition are strongly influenced by water content.

Nonplastic silts have been used successfully as cores for dams and for other fills. Their behavior during compaction is sensitive to water content, and they become rubbery when compacted close to saturation. In this condition they deform elastically under wheel loads, without failure and without further increase in density. Highly plastic silts, such as San Francisco Bay mud, have also been used as fills, but adjusting the moisture contents of highly plastic materials to achieve the water content and the degree of compaction needed for a high-quality fill is difficult.

Evaluating Strengths of Natural Deposits of Silt

Plastic and nonplastic silts can be sampled using techniques that have been developed for clays, although the quality of the samples is not as good. Disturbance during sampling is a problem for all silts, and care to minimize disturbance effects is important, especially for samples used to measure undrained strengths. Sample disturbance has a much smaller effect on measured values of the effective stress friction angle (ϕ') than it has on undrained strength.

Effective stress failure envelopes for silts can be determined readily using consolidated–undrained triaxial tests with pore pressure measurements, using test specimens trimmed from "undisturbed" samples. Drained direct shear tests can also be used. Drainage may occur so slowly in triaxial tests that performing drained triaxial tests may be impractical as a means of measuring drained strengths.

Correlations are not available for making reliable estimates of the undrained strengths of silts, because values of s_u/σ'_{1c} measured for different silts vary widely. A few examples are shown in Table 5.5.

Table 5.5 Values of s_u/σ'_{1c} for Normally Consolidated Alaskan Silts

Test[a]	k_c[b]	s_u/σ'_{1c}	Reference
UU	NA	0.25–0.30	Fleming and Duncan (1990)
UU	NA	0.18	Jamiolkowski et al. (1985)
IC-U	1.0	0.25	Jamiolkowski et al. (1985)
IC-U	1.0	0.30	Jamiolkowski et al. (1985)
IC-U	1.0	0.85–1.0	Fleming and Duncan (1990)
IC-U	1.0	0.30–0.65	Wang and Vivatrat (1982)
AC-U	0.84	0.32	Jamiolkowski et al. (1985)
AC-U	0.59	0.39	Jamiolkowski et al. (1985)
AC-U	0.59	0.26	Jamiolkowski et al. (1985)
AC-U	0.50	0.75	Fleming and Duncan (1990)

[a]UU, unconsolidated undrained triaxial; IC-U, isotropically consolidated undrained triaxial; AC-U, anisotropically consolidated undrained triaxial.

[b]$k_c = \sigma'_{3c}/\sigma'_{1c}$ during consolidation.

Additional studies will be needed to develop more refined methods of classifying silts and correlations that can be used to make reliable estimates of undrained strengths. Until more information is available, properties of silts should be based on conservative lower-bound estimates, or laboratory tests on the specific material.

Recapitulation

- The behavior of silts has not been studied as extensively, and is not as well understood, as the behavior of granular materials and clays.
- It is often difficult to determine whether silts will be drained or undrained under field loading conditions. In many cases it is prudent to consider both possibilities.
- Silts encompass a broad range of behavior, from fine sands to clays. It is useful to consider silts in two categories: nonplastic silts, which behave more like fine sands, and plastic silts, which behave like clays.
- Disturbance during sampling is a serious problem in nonplastic silts.
- Cavitation may occur during tests on nonplastic silts, forming bubbles within test specimens that greatly affect their behavior.
- Correlations are not available for making reliable estimates of the undrained strengths of silts.
- Laboratory test programs for silts to be used as fills can be conducted following the principles that have been established for testing clays.

CLAYS

Through their complex interactions with water, clays are responsible for a large percentage of problems with slope stability. The strength properties of clays are complex and subject to changes over time through consolidation, swelling, weathering, development of slickensides, and creep. Undrained strengths of clays are important for short-term loading conditions, and drained strengths are important for long-term conditions.

The shear strength of clays in terms of effective stress can be expressed by the Mohr-Coulomb strength criterion as

$$s = c' + \sigma' \tan \phi' \tag{5.6}$$

where s is the shear strength, c' the effective stress cohesion intercept, and ϕ' the effective stress angle of internal friction.

The shear strength of clays in terms of total stress can be expressed as

$$s = c + \sigma \tan \phi \tag{5.7}$$

where c and ϕ are the total stress cohesion intercept and the total stress friction angle.

For saturated clays, ϕ is equal to zero, and the undrained strength can be expressed as

$$s = s_u = c \tag{5.8a}$$

$$\phi = \phi_u = 0 \tag{5.8b}$$

where s_u is the undrained shear strength, independent of total normal stress, and ϕ_u is the total stress friction angle.

Factors Affecting Clay Strength

Low undrained strengths of normally consolidated and moderately overconsolidated clays cause frequent problems with stability of embankments constructed on them. Accurate evaluation of undrained strength, a critical factor in evaluating stability, is difficult because so many factors influence the results of laboratory and in situ tests for clays.

Disturbance. Sample disturbance reduces strengths measured in unconsolidated–undrained (UU) tests in the laboratory. Strengths measured using UU tests may be considerably lower than the undrained strength in situ unless the samples are of high quality. Two procedures have been developed to mitigate disturbance effects (Jamiolkowski et al., 1985):

1. The *recompression technique,* described by Bjerrum (1973), involves consolidating specimens in the laboratory at the same pressures to which they were consolidated in the field. This replaces the field effective stresses with the same effective stresses in the laboratory and squeezes out extra water that the sample may have absorbed as it was sampled, trimmed, and set up in the triaxial cell. This method is used extensively in Norway to evaluate undrained strengths of the sensitive marine clays found there.
2. The *SHANSEP technique,* described by Ladd and Foott (1974) and Ladd et al. (1977), involves consolidating samples to effective stresses that are higher than the in situ stresses, and interpreting the measured strengths in terms of the undrained strength ratio, s_u/σ'_v. Variations of s_u/σ'_v with OCR for six clays, determined from this type of testing, are shown in Figure 5.11. Data of the type shown in Figure 5.11, together with knowledge of the variations of σ'_v and OCR with

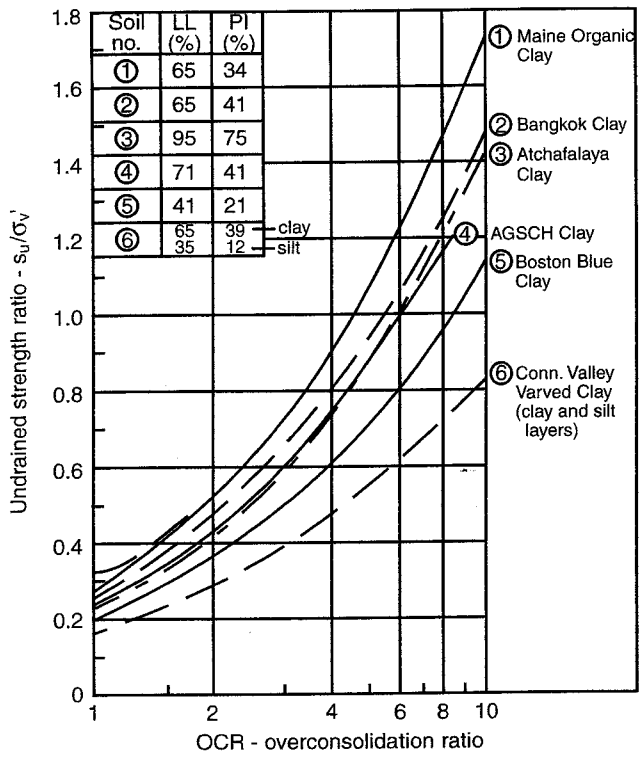

Figure 5.11 Variation of s_u/σ_v' with OCR for clays, measured in ACU direct simple shear tests. (After Ladd et al., 1977.)

depth, can be used to estimate undrained strengths for deposits of normally consolidated and moderately overconsolidated clays.

As indicated by Jamiolkowski et al. (1985), both the recompression and the SHANSEP techniques have limitations. The recompression technique is preferable whenever block samples (with very little disturbance) are available. It may lead to undrained strengths that are too low if the clay has a delicate structure that is subject to disturbance as a result of even very small strains (these are called *structured clays*), and it may lead to undrained strengths that are too high if the clay is less sensitive, because reconsolidation results in void ratios in the laboratory that are lower than those in the field. The SHANSEP technique is applicable only to clays without sensitive structure, for which undrained strength increases in direct proportion to the consolidation pressure. It requires detailed knowledge of past and present in situ stress conditions, because the undrained strength profile is constructed using data such as those shown in Figure 5.11, based on knowledge of σ_v' and OCR.

Anisotropy. The undrained strength of clays is *anisotopic;* that is, it varies with the orientation of the failure plane. Anisotropy in clays is due to two effects: inherent anisotropy and stress system-induced anisotropy.

Inherent anisotropy in intact clays results from the fact that plate-shaped clay particles tend to become oriented perpendicular to the major prinicpal strain direction during consolidation, which results in direction-dependent stiffness and strength. Inherent anisotropy in stiff-fissured clays also results from the fact that fissures are planes of weakness.

Stress system-induced anisotropy is due to the fact that the magnitudes of the stresses during consolidation vary depending on the orientation of the planes on which they act, and the magnitudes of the pore pressures induced by undrained loading vary with the orientation of the changes in stress.

The combined result of inherent and stress-induced anisotropy is that the undrained strengths of clays varies with the orientation of the principal stress at failure and with the orientation of the failure plane. Figure 5.12*a* shows orientations of principal stresses and failure planes around a shear surface. Near the top of the shear surface, sometimes called the *active zone,* the

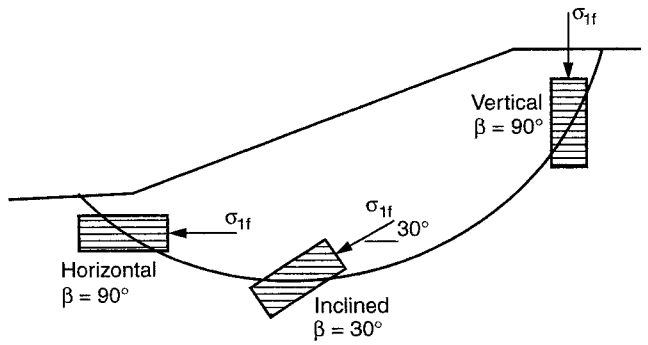

(*a*)

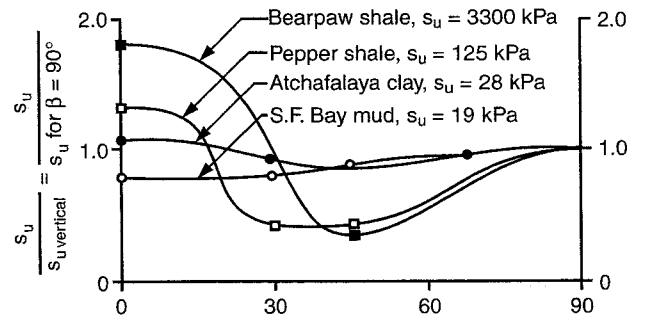

(*b*)

Figure 5.12 Stress orientation at failure, and undrained strength anisotropy of clays and shales: (*a*) stress orientations at failure; (*b*) anisotropy of clays and shales—UU triaxial tests.

major principal stress at failure is vertical, and the shear surface is oriented about 60° from horizontal. In the middle part of the shear surface, where the shear surface is horizontal, the major principal stress at failure is oriented about 30° from horizontal. At the toe of the slope, sometimes called the *passive zone,* the major principal stress at failure is horizontal, and the shear surface is inclined about 30° past horizontal. As a result of these differences in orientation, the undrained strength ratio (s_u/σ_v') varies from point to point around the shear surface. Variations of undrained strengths with orientation of the applied stress in the laboratory are shown in Figure 5.12*b* for two normally consolidated clays and two heavily overconsolidated clay shales.

Ideally, laboratory tests to measure the undrained strength of clay would be performed on completely undisturbed plane strain test specimens, tested under unconsolidated–undrained conditions, or consolidated and sheared with stress orientations that simulate those in the field. However, equipment that can apply and reorient stresses to simulate these effects is highly complex and has been used only for research purposes. For practical applications, tests must be performed with equipment that is easier to use, even though it may not replicate all the various aspects of the field conditions.

Triaxial compression (TC) tests, often used to simulate conditions at the top of the slip surface, have been found to result in strengths that are 5 to 10% lower than vertical compression plane strain tests. Triaxial extension (TE) tests, often used to simulate conditions at the bottom of the slip surface, have been found to result in strengths that are significantly less (at least 20% less) than strengths measured in horizontal compression plane strain tests. Direct simple shear (DSS) tests, often used to simulate the condition in the central portion of the shear surface, underestimate the undrained shear strength on the horizontal plane. As a result of these biases, the practice of using TC, TE, and DSS tests to measure the undrained strengths of normally consolidated clays results in strengths that are lower than the strengths that would be measured in ideally oriented plane strain tests.

Strain rate. Laboratory tests involve higher rates of strain than are typical for most field conditions. UU test specimens are loaded to failure in 10 to 20 minutes, and the duration of CU tests is usually 2 or 3 hours. Field vane shear tests are conducted in 15 minutes or less. Loading in the field, on the other hand, typically involves a period of weeks or months. The difference in these loading times is on the order of 1000. Slower loading results in lower undrained shear strengths of saturated clays. As shown in Figure 5.13, the strength of San Francisco Bay mud decreases by about 30% as the time to failure increases from 10 minutes to 1 week. It appears that there is no further decrease in undrained strength for longer times to failure.

In conventional practice, laboratory tests are not corrected for strain rate effects or disturbance effects. Because high strain rates increase strengths measured in UU tests and disturbance reduces them, these effects tend to cancel each other when UU laboratory tests are used to evaluate undrained strengths of natural deposits of clay.

Methods of Evaluating Undrained Strengths of Intact Clays

Alternatives for measuring or estimating undrained strengths of normally consolidated and moderately ov-

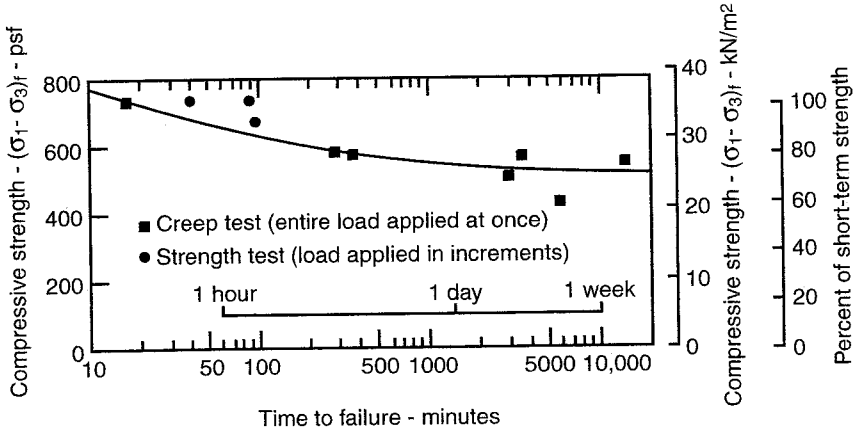

Figure 5.13 Strength loss due to sustained loading.

erconsolidated clays are summarized in Table 5.6. Samples used to measure strengths of natural deposits of clay should be as nearly undisturbed as possible. Hvorslev (1949) has detailed the requirements for good sampling, which include (1) use of thin-walled tube samplers (wall area no more than about 10% of sample area), (2) a piston inside the tube to minimize strains in the clay as the sample tube is inserted, (3) sealing samples after retrieval to prevent change in water content, and (4) transportation and storage procedures that protect the samples from shock, vibration, and excessive temperature changes. Block samples, carefully trimmed and sealed in moistureproof material, are the best possible types of sample. The consequence of poor sampling is scattered and possibly misleading data. One test on a good sample is better than 10 tests on poor samples.

Field vane shear tests. When the results of field vane shear tests are corrected for strain rate and anisotropy effects, they provide an effective method of measuring the undrained strength of soft and medium clays in situ. Bjerrum (1972) developed correction factors for vane shear tests by comparing field vane (FV) strengths with strengths back-calculated from slope failures. The value of the correction factor, μ, varies with the plasticity index, as shown in Figure 5.14. The data that form the basis for these corrections are rather widely scattered, and vane strengths should not be viewed as precise, even after correction. Nevertheless, the vane shear test avoids many of the problems involved in sampling and laboratory testing and has been found to be a useful tool for measuring the undrained strengths of normally consolidated and moderately overconsolidated clays.

Table 5.6 Methods of Measuring or Estimating the Undrained Strengths of Clays

Procedure	Comments
UU tests on vertical, inclined, and horizontal specimens to determine variation of undrained strength with direction of compression	Relies on counterbalancing effects of disturbance and creep. Empirical method of accounting for anisotropy gives results in agreement with vertical and horizontal plane strain compression tests for San Francisco Bay mud and with field behavior of Pepper shale.
AC-U triaxial compression, triaxial extension, and direct simple shear tests, using the recompression or SHANSEP technique	All three tests give lower undrained strengths than the ideal oriented plane strain tests they approximate. Creep strength loss tends to counterbalance these low strengths.
Field vane shear tests, corrected using empirical correction factors (see Figure 5.14)	Correction accounts for anisotropy and creep strength loss. The data on which the correction factor is based contain considerable scatter.
Cone penetration tests, with an empirical cone factor to evaluate undrained strength (see Figure 5.15)	Empirical cone factors can be determined by comparison with corrected vane strengths or estimated based on published data. Strengths based on CPT results involve at least as much uncertainty as strengths based on vane shear tests.
Standard Penetration Tests, with an empirical factor to evaluate undrained strength (see Figure 5.16)	The Standard Penetration Test is not a sensitive measure of undrained strengths in clays. Strengths based on SPT results involve a great deal of uncertainty.
Use $s_u = [0.23(\mathrm{OCR})^{0.8}]\sigma'_v$	This empirical formula, suggested by Jamiolkowski et al. (1985), reflects the influence of σ'_v (effective overburden pressure) and OCR (overconsolidation ratio), but merely approximates the average of the undrained strengths shown in Figure 5.11. The strengths of particular clays may be higher or lower.
Use $s_u = 0.22\sigma'_p$	This empirical formula, suggested by Mesri (1989) combines the influence of σ'_v and OCR in σ'_p (preconsolidation pressure), resulting in a simpler expression. The degree of approximation is essentially the same as for the formula suggested by Jamiolkowski et al. (1985).

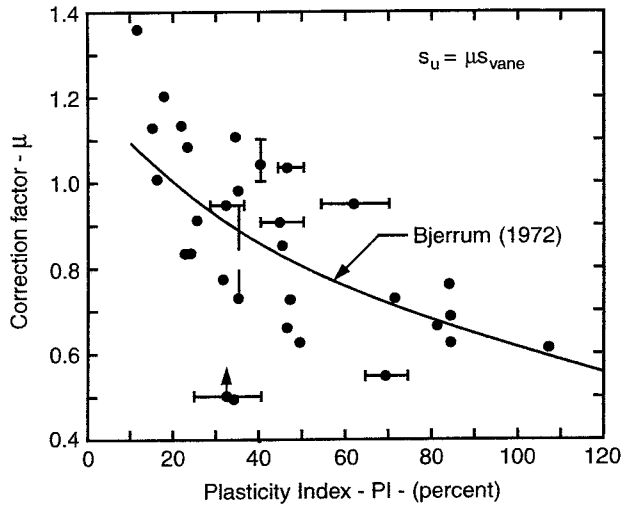

Figure 5.14 Variation of vane shear correction factor and plasticity index. (After Ladd et al., 1977.)

Cone penetration tests. Cone penetration tests (CPTs) are attractive as a means of evaluating undrained strengths of clays in situ because they can be performed quickly and at lower cost than field vane shear tests. The relationship between undrained strength and cone tip resistance is

$$s_u = \frac{q_c - \sigma_{vo}}{N_k^*} \tag{5.9}$$

where s_u is the undrained shear strength, q_c the CPT tip resistance, σ_v the total overburden pressure at the test depth, and N_k^* the cone factor. The units for s_u, q_c, and σ_v in Eq. (5.9) must be the same.

Values of the cone factor N_k^* for a number of different clays are shown in Figure 5.15. These values were developed by comparing *corrected* vane strengths with cone penetration resistance. Therefore Eq. (5.9) provides values of s_u comparable to values determined from field vane shear tests *after correction*. It can be seen that there is little systematic variation of N_k^* with the plasticity index. A value of $N_k^* = 14 \pm 5$ is applicable to clays with any PI value.

A combination of field vane shear and CPT tests can often be used to good advantage to evaluate undrained strengths at soft clay sites. A few vane shear tests are performed close to CPT test locations, and a site-specific value of N_k^* is determined by comparing the results. The cone test is then used for production testing.

Standard Penetration Tests. Undrained strengths can be estimated very crudely based on the results of Standard Penetration Tests. Figure 5.16, which shows

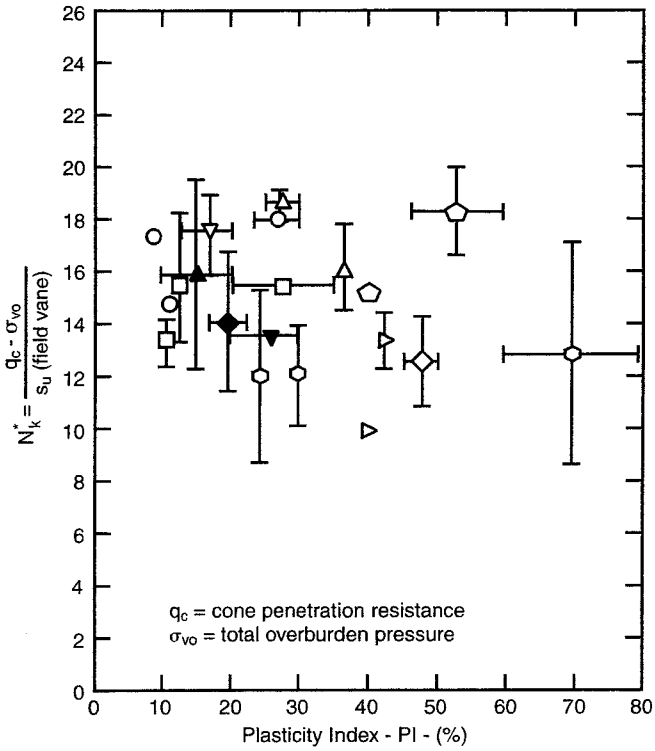

Figure 5.15 Variation of the ratio of net cone resistance ($q_c - \sigma_{vo}$) divided by vane shear strength (s_u vane) with plasticity index for clays. (After Lunne and Klevan, 1982.)

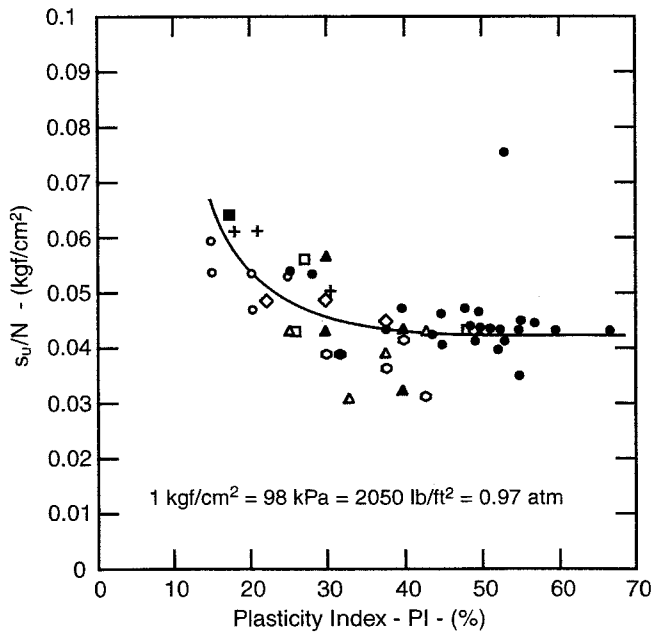

Figure 5.16 Variation of the ratio of undrained shear strength (s_u) divided by SPT blow count (N), with plasticity index for clay. (After Terzaghi et al., 1996.)

the variation of s_u/N with Plasticity Index, can be used to estimate undrained strength based on SPT blow count. In Figure 5.16 the value of s_u is expressed in kgf/cm^2 (1.0 kgf/cm^2 is equal to 98 kPa, or 1.0 ton per square foot). The Standard Penetration Test is not a sensitive indicator of the undrained strength of clays, and it is not surprising that there is considerable scatter in the correlation shown in Figure 5.16.

Typical Peak Friction Angles for Intact Clays

Tests to measure peak drained strengths of clays include drained direct shear tests and triaxial tests with pore pressure measurements to determine c' and ϕ'. The tests should be performed on undisturbed test specimens. Typical values of ϕ' for normally consolidated clays are given in Table 5.7. Strength envelopes for normally consolidated clays go through the origin of stresses, and $c' = 0$ for these materials.

Stiff-Fissured Clays

Heavily overconsolidated clays are usually stiff, and they usually contain fissures. The term *stiff-fissured clays* is often used to describe them. Terzaghi (1936) pointed out what has since been confirmed by many others—the strengths that can be mobilized in stiff-fissured clays in the field are less than the strength of the same material measured in the laboratory.

Skempton (1964, 1970, 1977, 1985), Bjerrum (1967), and others have shown that this discrepancy is due to swelling and softening that occurs in the field over long periods of time but does not occur in the laboratory within the period of time used to perform laboratory strength tests. A related factor is that fissures, which have an important effect on the strength of the clay in the field, are not properly represented in laboratory samples unless the test specimens are large enough to include a significant number of fissures. Unless the specimen size is several times the average fissure spacing, both drained and undrained strengths measured in laboratory tests will be too high.

Table 5.7 Typical Values of Peak Friction Angle (ϕ') for Normally Consolidated Clays[a]

Plasticity index	ϕ' (deg)
10	33 ± 5
20	31 ± 5
30	29 ± 5
40	27 ± 5
60	24 ± 5
80	22 ± 5

Source: Data from Bjerrum and Simons (1960).
[a] $c' = 0$ for these materials.

Peak, fully softened, and residual strengths of stiff-fissured clays. Skempton (1964, 1970, 1977, 1985) investigated a number of slope failures in the stiff-fissured London clay and developed procedures for evaluating the drained strengths of stiff-fissured clays that have been widely accepted. Figure 5.17 shows stress–displacement curves and strength envelopes for drained direct shear tests on stiff-fissured clays. The undisturbed peak strength is the strength of undisturbed test specimens from the field. The magnitude of the cohesion intercept (c') depends on the size of the test specimens. Generally, the larger the test specimens, the smaller the value of c'. As displacement continues beyond the peak, reached at $\Delta x = 0.1$ to 0.25 in. (3 to 6 mm), the shearing resistance decreases. At displacements of 10 in. (250 mm) or so, the shearing resistance decreases to a residual value. In clays without coarse particles, the decline to residual strength is accompanied by formation of a slickensided surface along the shear plane.

If the same clay is remolded, mixed with enough water to raise its water content to the liquid limit, consolidated in the shear box, and then tested, its peak strength will be lower than the undisturbed peak. The strength after remolding and reconsolidating is shown by the NC (normally consolidated) stress–displacement curve and shear strength envelope. The peak is less pronounced, and the NC strength envelope passes through the origin, with c' equal to zero. As shearing displacement increases, the shearing resistance decreases to the same residual value as in the test on the undisturbed test specimen. The displacement required to reach the residual shearing resistance is again about 10 in. (250 mm).

Studies by Terzaghi (1936), Henkel (1957), Skempton (1964), Bjerrum (1967), and others have shown that factors of safety calculated using undisturbed peak strengths for slopes in stiff-fissured clays are larger than unity for slopes that have failed. It is clear, therefore, that laboratory tests on undisturbed test specimens do not result in strengths that can be used to evaluate the stability of slopes in the field.

Skempton (1970) suggested that this discrepancy is due to the fact that more swelling and softening occurs in the field than in the laboratory. He showed that the NC peak strength, also called the *fully softened strength,* corresponds to strengths back-calculated from *first-time slides,* slides that occur where there is no preexisting slickensided failure surface. Skempton also

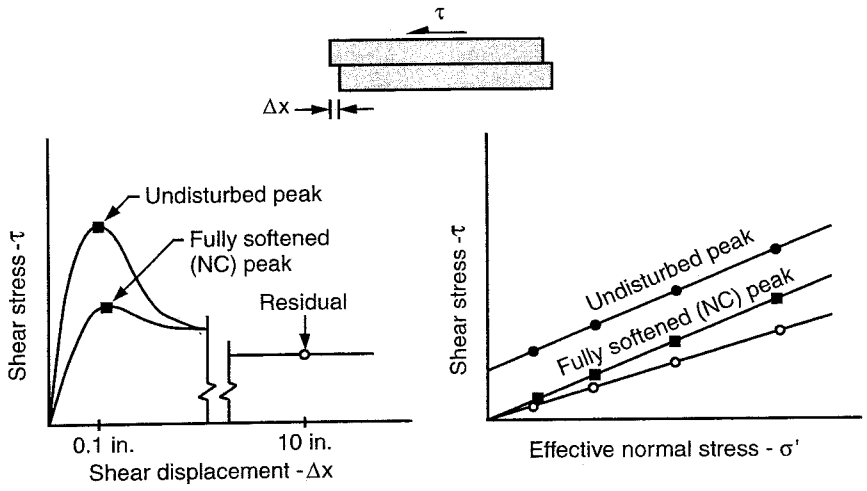

Figure 5.17 Drained shear strength of stiff fissured clay.

showed that once a failure has occurred and a continuous slickensided failure surface has developed, only the residual shear strength is available to resist sliding. Tests to measure fully softened and residual drained strengths of stiff clays can be performed using any representative sample, disturbed or undisturbed, because they are performed on remolded test specimens.

Direct shear tests have been used to measure fully softened and residual strengths. They are more suitable for measuring fully softened strengths because the displacement required to mobilize the fully softened peak strength is small, usually about 0.1 to 0.25 in. (2.5 to 6 mm). Direct shear tests are not so suitable for measuring residual strengths because it is necessary to displace the top of the shear box back and forth to accumulate sufficient displacement to develop a slickensided surface on the shear plane and reduce the shear strength to its residual value. Ring shear tests (Stark and Eid, 1993) are preferable for measuring residual shear strengths because unlimited shear displacement is possible through continuous rotation.

Figures 5.18 and 5.19 show correlations of fully softened friction angle and residual friction angle with liquid limit, clay-size fraction, and effective normal

400 kPA = 4.17 tsf
50 kPA = 0.522 tsf

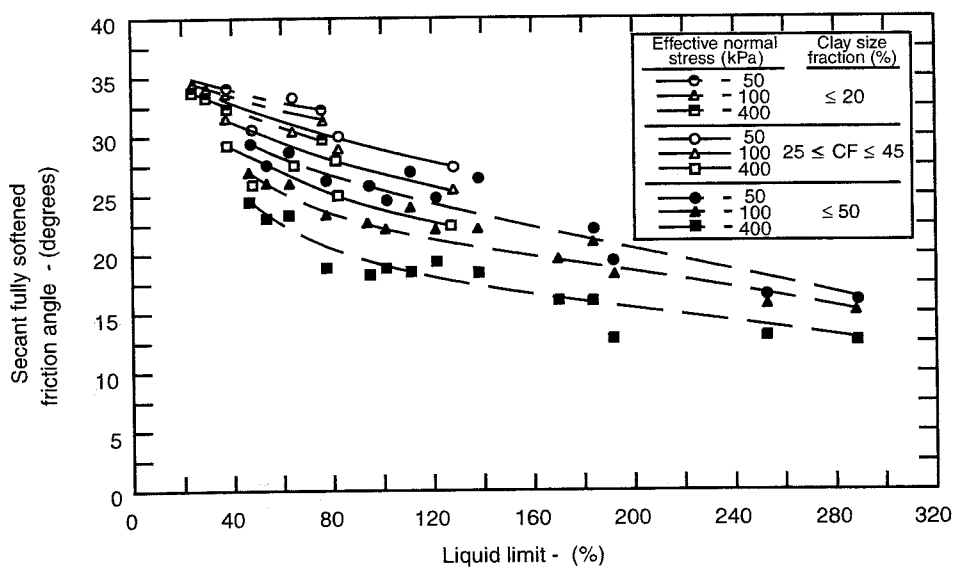

Figure 5.18 Correlation among liquid limit, clay size fraction, and fully softened friction angle. (From Stark and Eid, 1997.)

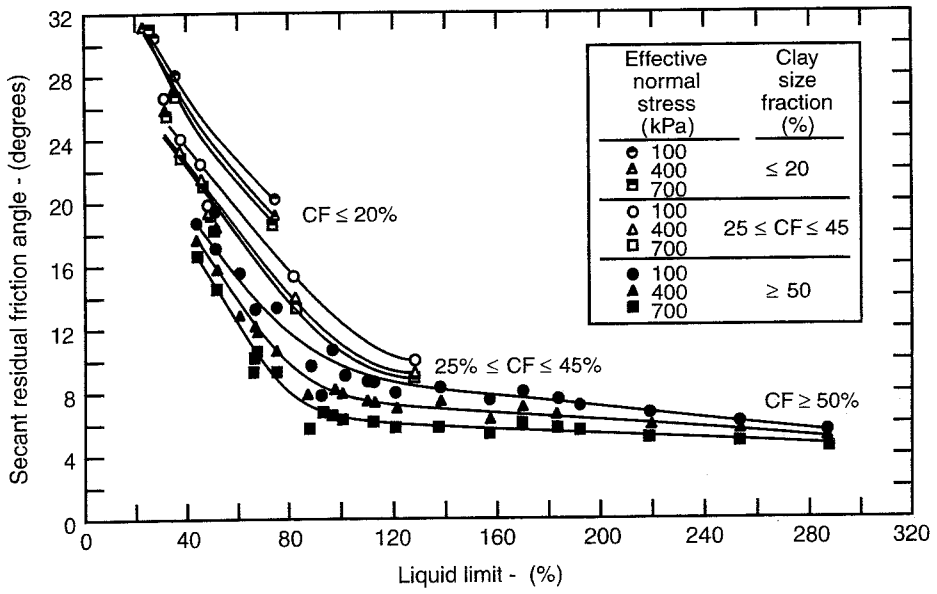

Figure 5.19 Correlation among liquid limit, clay size fraction, and residual friction angle. (From Stark and Eid, 1994.)

stress that were developed by Stark and Eid (1994, 1997). Both fully softened and residual friction angle are fundamental soil properties, and the correlations shown in Figures 5.18 and 5.19 have little scatter. Effective normal stress is a factor because the fully softened and residual strength envelopes are curved, as are the strength envelopes for granular materials. It is thus necessary to represent these strengths using nonlinear relationships between shear strength and normal stress, or to select values of ϕ' that are appropriate for the range of effective stresses in the conditions analyzed.

Undrained strengths of stiff-fissured clays. The undrained strength of stiff-fissured clays is also affected by fissures. Peterson et al. (1957) and Wright and Duncan (1972) showed that the undrained strengths of stiff-fissured clays and shales decreased as test specimen size increased. Small specimens are likely to be intact, with few or no fissures, and therefore stronger than a representative mass of the fissured clay. Heavily overconsolidated stiff fissured clays and shales are also highly anisotropic. As shown in Figure 5.12, inclined specimens of Pepper shale and Bearpaw shale, where

Table 5.8 Typical Peak Drained Strengths for Compacted Cohesive Soils

Unified classification	Relative compaction, RC[a] (%)	Effective stress cohesion, c' (kPa)	Effective stress friction angle, ϕ' (deg)
SM-SC	100	15	33
SC	100	12	31
ML	100	9	32
CL-ML	100	23	32
CL	100	14	28
MH	100	21	25
CH	100	12	19

Source: After U.S. Dept. Interior (1973).

[a]RC, relative compaction by USBR standard method, same energy as the Standard Proctor compaction test.

failure occurs on horizontal planes, are only 30 to 40% of the strengths of vertical specimens.

Compacted Clays

Compacted clays are used often to construct embankment dams, highway embankments, and fills to support buildings. When compacted well, at suitable water content, clay fills have high strength. Clays are more difficult to compact than are cohesionless fills. It is necessary to maintain their moisture contents during compaction within a narrow range to achieve good compaction, and more equipment passes are needed to produce high-quality fills. High pore pressures can develop in fills that are compacted wet of optimum, and stability during construction can be a problem in wet fills. Long-term stability can also be a problem, particularly with highly plastic clays, which are subject to swell and strength loss over time. It is necessary to consider both short- and long-term stability of compacted fill slopes in clay.

Drained strengths of compacted clays. Values of c' and ϕ' for compacted clays can be measured using consolidated–undrained triaxial tests with pore pressure measurements or drained direct shear tests. The values determined from either type of test are the same for practical purposes. The effective stress strength parameters for compacted clays, measured using samples that have been saturated before testing, are not strongly affected by compaction water content.

Table 5.8 lists typical values of c' and ϕ' for cohesive soils compacted to RC = 100% of the Standard Proctor maximum dry density. As the value of RC decreases below 100%, values of ϕ' remain about the same, and the value of c' decreases. For RC = 90%, values of c' are about half the values shown in Table 5.8.

Recapitulation

- The shear strength of clays in terms of effective stress can be expressed by the Mohr–Coulomb strength criterion as $s = c' + \sigma' \tan \phi'$.
- The shear strength of clays in terms of total stress can be expressed as $s = c + \sigma \tan \phi$.
- For saturated clays, ϕ is zero, and the undrained strength can be expressed as $s = s_u = c$, $\phi = \phi_u = 0$.
- Samples used to measure undrained strengths of normally consolidated and moderately overconsolidated clay should be as nearly undisturbed as possible.
- The strengths that can be mobilized in stiff fissured clays in the field are less than the strength of the same material measured in the laboratory using undisturbed test specimens.
- The normally consolidated peak strength, also called the fully softened strength, corresponds to strengths back calculated from first-time slides.
- Once a failure has occurred and a continuous slickensided failure surface has developed, only the residual shear strength is available to resist sliding.
- Tests to measure fully softened and residual drained strengths of stiff clays can be performed on remolded test specimens.
- Ring shear tests are preferable for measuring residual shear strengths, because unlimited shear displacement is possible through continuous rotation.
- Values of c' and ϕ' for compacted clays can be measured using consolidated–undrained triaxial tests with pore pressure measurements or drained direct shear tests.
- Undrained strengths of compacted clays vary with compaction water content and density and can be measured using UU triaxial tests performed on specimens at their as-compacted water contents and densities.

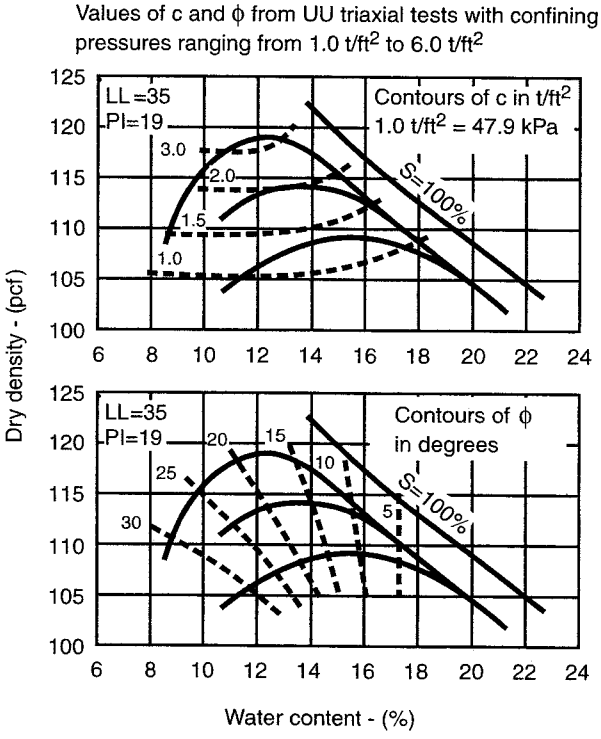

Figure 5.20 Strength parameters for compacted Pittsburgh sandy clay tested under UU test conditions. (From Kulhawy et al., 1969.)

Undrained strengths of compacted clays. Values of c and ϕ (total stress shear strength parameters) for the as-compacted condition can be determined by performing UU triaxial tests on specimens at their compaction water contents. Undrained strength envelopes for compacted, partially saturated clays tested are curved, as discussed in Chapter 3. Over a given range of stresses, however, a curved strength envelope can be approximated by a straight line and can be characterized in terms of c and ϕ. When this is done, it is especially important that the range of pressures used in the tests correspond to the range of pressures in the field conditions being evaluated. Alternatively, if the computer program used accommodates nonlinear strength envelopes, the strength test data can be represented directly.

Values of total stress c and ϕ for compacted clays vary with compaction water content and density. An example is shown in Figure 5.20 for compacted Pittsburgh sandy clay. The range of confining pressures used in these tests was 1.0 to 6.0 tons/ft^2. The value of c, the total stress cohesion intercept from UU tests, increases with dry density but is not much affected by compaction water content. The value of ϕ, the total stress friction angle, decreases as compaction water content increases, but is not so strongly affected by dry density.

If compacted clays are allowed to age prior to testing, they become stronger, apparently due to thixotropic effects. Therefore, undrained strengths measured using freshly compacted laboratory test specimens provide a conservative estimate of the strength of the fill a few weeks or months after compaction.

MUNICIPAL SOLID WASTE

Waste materials have strengths comparable to the strengths of soils. Strengths of waste materials vary depending on the amounts of soil and sludge in the waste, as compared to the amounts of plastic and other materials that tend to interlock and provide tensile strength (Eid et al., 2000). Larger amounts of materials that interlock increase the strength of the waste. Although solid waste tends to decompose or degrade with time, Kavazanjian (2001) indicates that the strength after degradation is similar to the strength before degradation.

Kavazanjian et al. (1995) used laboratory test data and back analysis of stable slopes to develop the lower-bound strength envelope for municipal solid waste shown in Figure 5.21. The envelope is horizontal with a constant strength c = 24 kPa, ϕ = 0 at normal pressures less than 37 kPa. At pressures greater than 37 kPa, the envelope is inclined at ϕ = 33° with c = 0.

Eid et al. (2000) used results of large-scale direct shear tests (300 to 1500 mm shear boxes) and back analysis of failed slopes in waste to develop the range of strength envelopes show in Figure 5.22. All three envelopes (lower bound, average, and upper bound) are inclined at ϕ = 35°. The average envelope shown in Figure 5.22 corresponds to c = 25 kPa, and the lowest of the envelopes corresponds to c = 0.

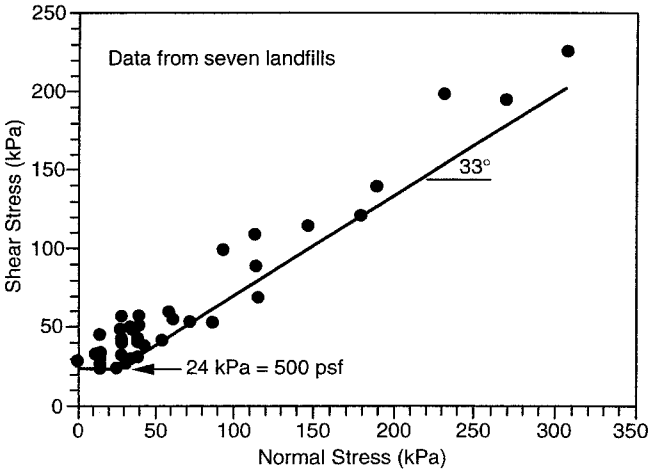

Figure 5.21 Shear strength envelope for municipal solid waste based on large-scale direct shear tests and back analysis of stable slopes. (After Kavazanjian et al., 1995.)

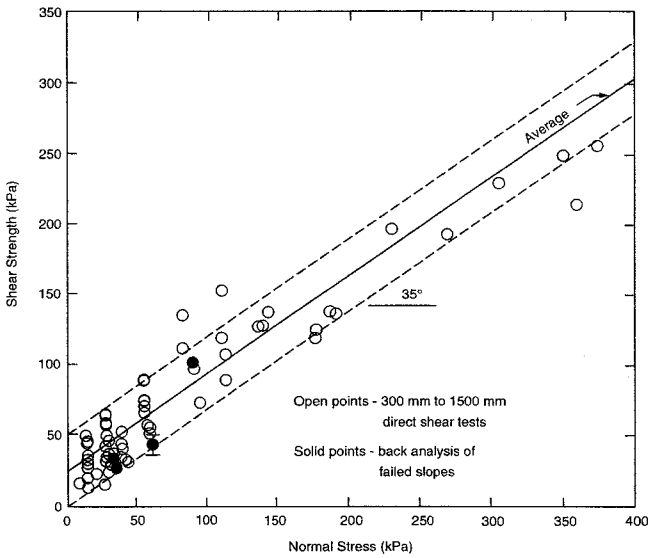

Figure 5.22 Range of shear strength envelopes for municipal solid waste based on large-scale direct shear tests and back analysis of failed slopes. (After Eid et al., 2000.)

CHAPTER 7

Methods of Analyzing Slope Stability

Methods for analyzing stability of slopes include simple equations, charts, spreadsheet software, and slope stability computer programs. In many cases more than one method can be used to evaluate the stability for a particular slope. For example, simple equations or charts may be used to make a preliminary estimate of slope stability, and later, a computer program may be used for detailed analyses. Also, if a computer program is used, another computer program, slope stability charts, or a spreadsheet should be used to verify results. The various methods used to compute a factor of safety are presented in this chapter.

SIMPLE METHODS OF ANALYSIS

The simplest methods of analysis employ a single simple algebraic equation to compute the factor of safety. These equations require at most a hand calculator to solve. Such simple equations exist for computing the stability of a vertical slope in purely cohesive soil, of an embankment on a much weaker, deep foundation, and of an infinite slope. Some of these methods, such as the method for computing the stability of an infinite slope, may provide a rigorous solution, whereas others, such as the equations used to estimate the stability of a vertical slope, represent some degree of approximation. Several simple methods are described below.

Vertical Slope in Cohesive Soil

For a vertical slope in cohesive soil a simple expression for the factor of safety is obtained based on a planar slip surface like the one shown in Figure 7.1. The average shear stress, τ, along the slip plane is expressed as

$$\tau = \frac{W \sin \alpha}{l} = \frac{W \sin \alpha}{H/\sin \alpha} = \frac{W \sin^2 \alpha}{H} \qquad (7.1)$$

where α is the inclination of the slip plane, H is the slope height, and W is the weight of the soil mass. The weight, W, is expressed as

$$W = \frac{1}{2} \frac{\gamma H^2}{\tan \alpha} \qquad (7.2)$$

which when substituted into Eq. (7.2) and rearranged gives

$$\tau = \tfrac{1}{2} \gamma H \sin \alpha \cos \alpha \qquad (7.3)$$

For a cohesive soil ($\phi = 0$) the factor of safety is expressed as

$$F = \frac{c}{\tau} = \frac{2c}{\gamma H \sin \alpha \cos \alpha} \qquad (7.4)$$

To find the minimum factor of safety, the inclination of the slip plane is varied. The minimum factor of safety is found for $\alpha = 45°$. Substituting this value for α (45°) into Eq. (7.4) gives

$$F = \frac{4c}{\gamma H} \qquad (7.5)$$

Equation (7.5) gives the factor of safety for a vertical slope in cohesive soil, assuming a plane slip surface. Circular slip surfaces give a slightly lower value for the factor of safety ($F = 3.83c/\gamma h$); however, the difference between the factors of safety based on a plane and a circular slip surface is small for a vertical slope in cohesive soil and can be ignored.

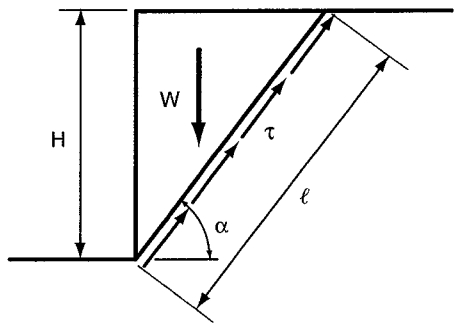

Figure 7.1 Vertical slope and plane slip surface.

Equation (7.5) can also be rearranged to calculate the critical height of a vertical slope (i.e., the height of a slope that has a factor of safety of unity). The critical height of a vertical slope in cohesive soil is

$$H_{\text{critical}} = \frac{4c}{\gamma} \tag{7.6}$$

Bearing Capacity Equations

The equations used to calculate the bearing capacity of foundations can also be used to estimate the stability of embankments on deep deposits of saturated clay. For a saturated clay and undrained loading ($\phi = 0$), the ultimate bearing capacity, q_{ult}, based on a circular slip surface is[1]

$$q_{\text{ult}} = 5.53c \tag{7.7}$$

Equating the ultimate bearing capacity to the load, $q = \gamma H$, produced by an embankment of height, H, gives

$$\gamma H = 5.53c \tag{7.8}$$

where γ is the unit weight of the soil in the embankment; γh represents the maximum vertical stress produced by the embankment. Equation (7.8) is an equilibrium equation corresponding to ultimate conditions (i.e., with the shear strength of the soil fully developed). If, instead, only some fraction of the shear strength is developed (i.e., the factor of safety is greater than unity), a factor of safety can be introduced into the equilibrium equation (7.8) and we can write

$$\gamma H = 5.53 \frac{c}{F} \tag{7.9}$$

In this equation F is the factor of safety with respect to shear strength; the term c/F represents the developed cohesion, c_d. Equation (7.9) can be rearranged to give

$$F = 5.53 \frac{c}{\gamma H} \tag{7.10}$$

Equation (7.10) can be used to estimate the factor of safety against a deep-seated failure of an embankment on soft clay.

Equation (7.10) gives a conservative estimate of the factor of safety of an embankment because it ignores the strength of the embankment and the depth of the foundation in comparison with the embankment width. Alternative bearing capacity equations that are applicable to reinforced embankments on thin clay foundations are presented in Chapter 8.

Infinite Slope

In Chapter 6 the equations for an infinite slope were presented. For these equations to be applicable, the depth of the slip surface must be small compared to the lateral extent of the slope. However, in the case of cohesionless soils, the factor of safety does not depend on the depth of the slip surface. It is possible for a slip surface to form at a small enough depth that the requirements for an infinite slope are met, regardless of the extent of the slope. Therefore, an infinite slope analysis is rigorous and valid for cohesionless slopes. The infinite slope analysis procedure is also applicable to other cases where the slip surface is parallel to the face of the slope and the depth of the slip surface is small compared to the lateral extent of the slope. This condition may exist where there is a stronger layer of soil at shallow depth: for example, where a layer of weathered soil exists near the surface of the slope and is underlain by stronger, unweathered material.

The general equation for the factor of safety for an infinite slope with the shear strength expressed in terms of total stresses is

$$F = \cot \beta \tan \phi + (\cot \beta + \tan \beta) \frac{c}{\gamma z} \tag{7.11}$$

[1] Although Prandtl's solution of $q_{\text{ult}} = 5.14c$ is commonly used for bearing capacity, it is more appropriate to use the solution based on circles, which gives a somewhat higher bearing capacity and offsets some of the inherent conservatism introduced when bearing capacity equations are applied to slope stability.

where z is the vertical depth of the slip surface below the face of the slope. For shear strengths expressed by effective stresses the equation for the factor of safety can be written as

$$F = \left[\cot \beta - \frac{u}{\gamma z}(\cot \beta + \tan \beta)\right] \tan \phi' + (\cot \beta + \tan \beta)\frac{c'}{\gamma z} \quad (7.12)$$

where u is the pore water pressure at the depth of the slip surface.

For effective stress analyses, Eq. (7.12) can also be written as

$$F = [\cot \beta - r_u (\cot \beta + \tan \beta)] \tan \phi' + (\cot \beta + \tan \beta) \frac{c'}{\gamma z} \quad (7.13)$$

where r_u is the pore pressure ratio defined by Bishop and Morgenstern (1960) as

$$r_u = \frac{u}{\gamma z} \quad (7.14)$$

Values of r_u can be determined for specific seepage conditions. For example, for seepage parallel to the slope, the pore pressure ratio, r_u, is given by

$$r_u = \frac{\gamma_w}{\gamma} \frac{h_w}{z} \cos^2 \beta \quad (7.15)$$

where h_w is the height of the free water surface vertically above the slip surface (Figure 7.2*a*). If the seepage exits the slope face at an angle (Figure 7.2*b*), the value of r_u is given by

$$r_u = \frac{\gamma_w}{\gamma} \frac{1}{1 + \tan \beta \tan \theta} \quad (7.16)$$

where θ is the angle between the direction of seepage (flow lines) and the horizontal. For the special case of horizontal seepage ($\theta = 0$), the expression for r_u reduces to

$$r_u = \frac{\gamma_w}{\gamma} \quad (7.17)$$

Recapitulation

- Simple equations can be used to compute the factor of safety for several slope and shear strength conditions, including a vertical slope in cohesive soil, an embankment on a deep deposit of saturated clay, and an infinite slope.
- Depending on the particular slope conditions and equations used, the accuracy ranges from excellent, (e.g., for a homogeneous slope in cohesionless soil) to relatively crude (e.g., for bearing capacity of an embankment on saturated clay).

SLOPE STABILITY CHARTS

The stability of many relatively homogeneous slopes can be calculated using slope stability charts based on one of the analysis procedures presented in Chapter 6. Fellenius (1936) was one of the first to recognize that factors of safety could be expressed by charts. His work was followed by the work of Taylor (1937) and Janbu (1954*b*). Since the pioneering work of these authors, numerous others have developed charts for computing the stability of slopes. However, the early charts of Janbu are still some of the most useful for many conditions, and these are described in further detail in the Appendix. The charts cover a range in slope and soil conditions and they are quite easy to use. In addition, the charts provide the minimum factor of safety and eliminate the need to search for a critical slip surface.

Stability charts rely on dimensionless relationships that exist between the factor of safety and other parameters that describe the slope geometry, soil shear strengths, and pore water pressures. For example, the infinite slope equation for effective stresses presented earlier [Eq. (7.13)] can be written as

$$F = [1 - r_u(1 + \tan^2 \beta)] \frac{\tan \phi'}{\tan \beta} + (1 + \tan^2 \beta) \frac{c'}{\gamma z} \quad (7.18)$$

or

$$F = A \frac{\tan \phi'}{\tan \beta} + B \frac{c'}{\gamma z} \quad (7.19)$$

where

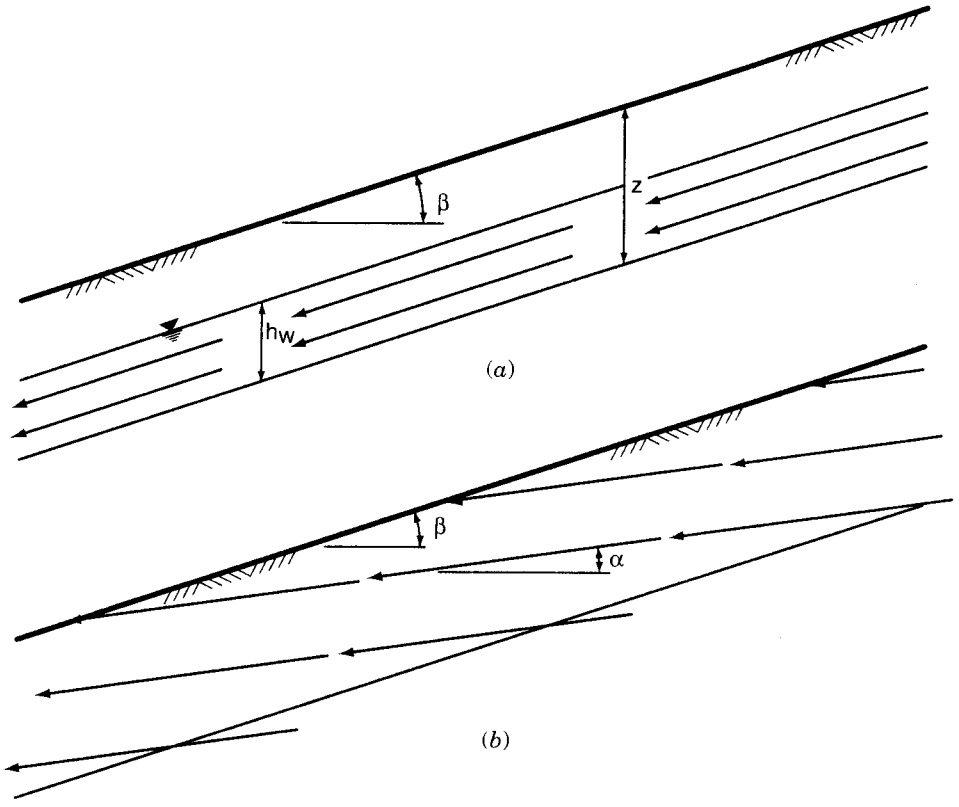

Figure 7.2 Infinite slope with seepage: (*a*) parallel to slope face; (*b*) exiting the slope face.

$$A = 1 - r_u(1 + \tan^2\beta) \tag{7.20}$$

$$B = 1 + \tan^2\beta \tag{7.21}$$

A and B are dimensionless parameters (*stability numbers*) that depend only on the slope angle, and in the case of A, the dimensionless pore water pressure coefficient, r_u. Simple charts for A and B as functions of the slope angle and pore water pressure coefficient, r_u, are presented in the Appendix.

For purely cohesive ($\phi = 0$) soils and homogeneous slopes, the factor of safety can be expressed as

$$F = N_0 \frac{c}{\gamma H} \tag{7.22}$$

where N_0 is a stability number that depends on the slope angle, and in the case of slopes flatter than about 1:1, on the depth of the foundation below the slope. For vertical slopes the value of N_0 according to the Swedish slip circle method is 3.83. This value (3.83) is slightly less than the value of 4 shown in Eq. (7.5) based on a plane slip surface. In general, circular slip surfaces give a lower factor of safety than a plane, especially for flat slopes. Therefore, circles are generally used for analysis of most slopes in cohesive soils. A complete set of charts for cohesive slopes of various inclinations and foundation depths is presented in the Appendix. Procedures are also presented for using average shear strengths with the charts when the shear strength varies.

For slopes with both cohesion and friction, additional dimensionless parameters are introduced. Janbu (1954) showed that the factor of safety could be expressed as

$$F = N_{cf} \frac{c'}{\gamma H} \tag{7.23}$$

where N_{cf} is a dimensionless stability number. The stability number depends on the slope angle, β, the pore water pressures, u, and the dimensionless parameter, $\lambda_{c\phi}$, which is defined as

$$\lambda_{c\phi} = \frac{\gamma H \tan\phi'}{c'} \tag{7.24}$$

Stability charts employing $\lambda_{c\phi}$ and Eq. (7.23) to calculate the factor of safety are presented in the Appen-

dix. These charts can be used for soils with cohesion and friction as well as a variety of pore water pressure and external surcharge conditions.

Although all slope stability charts are based on the assumption of constant shear strength (c, c' and ϕ, ϕ' are constant) or else a simple variation in undrained shear strength (e.g., c varies linearly with depth), the charts can be used for many cases where the shear strength varies. Procedures for using the charts for cases where the shear strength varies are described in the Appendix. Examples for using the charts are also presented in the Appendix.

Recapitulation

- Slope stability charts exist for computing the factor of safety for a variety of slopes and soil conditions.

SPREADSHEET SOFTWARE

Detailed computations for the procedures of slices can be performed in tabular form using a table where each row represents a particular slice and each column represents the variables and terms in the equations presented in Chapter 6. For example, for the case where $\phi = 0$ and the slip surface is a circle, the factor of safety is expressed as

$$F = \frac{\sum c\,\Delta l}{\sum W \sin \alpha} \tag{7.25}$$

A simple table for computing the factor of safety using Eq. (7.25) is shown in Figure 7.3. For the Ordinary Method of Slices with the shear strength expressed in terms of effective stresses, the preferred equation for computing the factor of safety is

$$F = \frac{\sum [c'\,\Delta l + (W \cos \alpha - u\,\Delta l \cos^2\alpha)\tan \phi']}{\sum W \sin \alpha} \tag{7.26}$$

A table for computing the factor of safety using this form of the Ordinary Method of Slices equation is illustrated in Figure 7.4. Tables such as the ones shown in Figures 7.3 and 7.4 are easily represented and implemented in computer spreadsheet software. In fact, more sophisticated tables and spreadsheets can be developed for computing the factor of safety using procedures of slices such as the Simplified Bishop, force equilibrium, and even Chen and Morgenstern's procedures (Low et al., 1998).

The number of different computer spreadsheets that have been developed and used to compute factors of safety is undoubtedly very large. This attests to the usefulness of spreadsheets for slope stability analyses, but at the same time presents several important problems: First, because such a large number of different spreadsheets are used and because each spreadsheet is often used only once or twice, it is difficult to validate spreadsheets for correctness. Also, because one person may write a spreadsheet, use it for some computations and then discard the spreadsheet, results are often poorly archived and difficult for someone else to interpret or to understand later. Electronic copies of the spreadsheet may have been discarded. Even if an electronic copy is maintained, the software that was used to create the spreadsheet may no longer be available or the software may have been updated such that the old spreadsheet cannot be accessed. Hard copies of numerical tabulations from the spreadsheet may have been saved, but unless the underlying equations, formulas, and logic that were used to create the numerical values are also clearly documented, it may be difficult to resolve inconsistencies or check for errors.

Recapitulation

- Spreadsheets provide a useful way of performing calculations by the procedures of slices.
- Spreadsheet calculations can be difficult to check and archive.

COMPUTER PROGRAMS

For more sophisticated analyses and complex slope, soil, and loading conditions, computer programs are generally used to perform the computations. Computer programs are available that can handle a wide variety of slope geometries, soil stratigraphies, soil shear strength, pore water pressure conditions, external loads, and internal soil reinforcement. Most programs also have capabilities for automatically searching for the most critical slip surface with the lowest factor of safety and can handle slip surfaces of both circular and noncircular shapes. Most programs also have graphics capabilities for displaying the input data and the results of the slope stability computations.

Types of Computer Programs

Two types of computer programs are available for slope stability analyses: The first type of computer program allows the user to specify as input data the slope geometry, soil properties, pore water pressure condi-

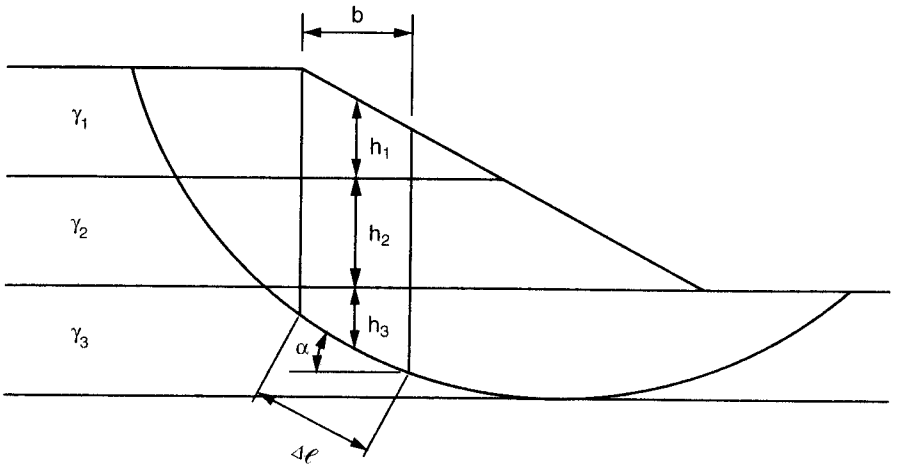

Slice No.	b	h_1	γ_1	h_2	γ_2	h_3	γ_3	$W^{(1)}$	α	$\Delta\ell^{(2)}$	c	$c\Delta\ell$	W sinα
1													
2													
3													
4													
5													
6													
7													
8													
9													
10													
										Summation:			

(1) $W = b \times (h_1\gamma_1 + h_2\gamma_2 + h_3\gamma_3)$
(2) $\Delta\ell = b / \cos\alpha$

$$F = \frac{\Sigma c\Delta\ell}{\Sigma W \sin\alpha}$$

Figure 7.3 Sample table for manual calculations using the Swedish circle ($\phi = 0$) procedure.

tions, external loads, and soil reinforcement, and computes a factor of safety for the prescribed set of conditions. These programs are referred to as *analysis programs*. They represent the more general type of slope stability computer program and are almost always based on one or more of the procedures of slices.

The second type of computer program is the *design program*. These programs are intended to determine what slope conditions are required to provide one or more factors of safety that the user specifies. Many of the computer programs used for reinforced slopes and other types of reinforced soil structures such as soil nailed walls are of this type. These programs allow the user to specify as input data general information about the slope geometry, such as slope height and external loads, along with the soil properties. The programs may also receive input on candidate reinforcement materials such as either the tensile strength of the reinforcement or even a particular manufacturer's product number along with various factors of safety to be achieved. The computer programs then determine what type and extent of reinforcement are required to produce suitable factors of safety. The design programs may be based on either procedures of slices or single-free-body procedures. For example, the logarithmic spiral procedure has been used in several computer

Slice No.	b	h_1	γ_1	h_2	γ_2	h_3	γ_3	W	$\Delta\ell$	α	c'	ϕ'	u	$u\Delta\ell$	W cosα	W cosα - $u\Delta\ell\cos^2\alpha$	(W cosα - $u\Delta\ell\cos^2\alpha$)tanϕ'	$c'\Delta\ell$	W sinα
1																			
2																			
3																			
4																			
5																			
6																			
7																			
8																			
9																			
10																			
															Summation:				

Note: 1. $W = b \times (h_1\gamma_1 + h_2\gamma_2 + h_3\gamma_3)$
2. $\Delta\ell = b / \cos\alpha$

$$F = \frac{\Sigma[(W\cos\alpha - u\Delta\ell\cos^2\alpha)\tan\phi' - c'\Delta\ell]}{\Sigma W\sin\alpha}$$

Figure 7.4 Sample table for manual calculations using the Ordinary Method of Slices and effective stresses.

programs for both geogrid and soil nail design (Leshchinsky, 1997; Byrne, 2003[2]). The logarithmic spiral procedure is very well suited for such applications where only one soil type may be considered in the cross section.

Design programs are especially useful for design of reinforced slopes using a specific type of reinforcement (e.g., geogrids or soil nails) and can eliminate much of the manual trial-and-error effort required. However, the design programs are usually restricted in the range of conditions that can be handled and they often make simplifying assumptions about the potential failure mechanisms. Most analysis program can handle a much wider range of slope and soil conditions.

Automatic Searches for Critical Slip Surface

Almost all computer programs employ one or more schemes for searching for a critical slip surface with the minimum factor of safety. Searches can be performed using both circular and noncircular slip surfaces. Usually, different schemes are used depending on the shape (circular vs. noncircular) of slip surface used. Many different search schemes have been used, and it is beyond the scope of this chapter to discuss these in detail. Nevertheless, several recommendations and guidelines can be offered for searching for a critical slip surface:

1. *Start with circles.* It is almost always preferable to begin searching for a critical slip surface using circles. Very robust schemes exist for searching with circles, and it is possible to examine a large number of possible locations for a slip surface with relatively little effort on the part of the user.
2. *Let stratigraphy guide the search.* For both circular and noncircular slip surfaces, the stratigraphy often suggests where the critical slip surface will be located. In particular, if a relatively weak zone exists, the critical slip surface is likely to pass through it. Similarly, if the weak zone is relatively thin and linear, the slip surface may follow the weak layer and is more likely to be noncircular than circular.
3. *Try multiple starting locations.* Almost all automatic searches begin with a slip surface that the user specifies in some way. Multiple starting locations should be tried to determine if one location leads to a lower factor of safety than another.

[2]Byrne has utilized the log spiral procedure in an unreleased version of the GoldNail software. One of the authors (Wright) has also used the log spiral successfully for this purpose in unreleased software for analyzing soil nail walls.

4. *Be aware of multiple minima.* Many search schemes are essentially optimization schemes that seek to find a single slip surface with the lowest factor of safety. However, there may be more than one "local" minimum and the search scheme may not necessarily find the local minimum that produces the lowest factor of safety overall. This is one of the reasons why it is important to use multiple starting locations for the search.
5. *Vary the search constraints and other parameters.* Most search schemes require one or more parameters that control how the search is performed. For example, some of the parameters that may be specified include:
   - The incremental distances that the slip surface is moved during the search
   - The maximum depth for the slip surface
   - The maximum lateral extent of the slip surface or search
   - The minimum depth or weight of soil mass above the slip surface
   - The maximum steepness of the slip surface where it exits the slope
   - The lowest coordinate allowed for the center of a circle (e.g., to prevent inversion of the circle)

   Input data should be varied to determine how these parameters affect the outcome of the search and the minimum factor of safety.

A relatively large number of examples and benchmarks can be found in the literature for the factor of safety for a particular slip surface. However, many fewer examples can be found to confirm the location of the most critical slip surface (lowest factor of safety), even though this may be the more important aspect of verification. For complex slopes, much more effort is usually spent in a slope stability analysis to verify that the most critical slip surface is found than is spent to verify that the factor of safety for a given slip surface has been computed correctly.

Restricting the Critical Slip Surfaces of Interest

In general, all areas of a slope should be searched to find the critical slip surface with the minimum factor of safety. However, is some cases it may be desirable to search only a certain area of the slope by restricting the location of trial slip surfaces. There are two common cases where this is appropriate. One case is where there are insignificant modes of failure that lead to low factors of safety, but the consequences of failure are small. The other case is where the slope geometry is such that a circle with a given center point and radius does not define a unique slip surface and slide mass. These two cases are described and discussed further below.

Insignificant modes of failure. For cohesionless slopes it has been shown that the critical slip surface is a very shallow plane, essentially coincident with the face of the slope. However, the consequences of a slide where only a thin layer of soil is involved may be very low and of little significance. This is particularly the case for some mine tailings disposal dams. In such cases it is desirable to investigate only slip surfaces that have some minimum size and extent. This can be done in several ways, depending on the particular computer program being used:

- The slip surfaces investigated can be required to have a minimum depth.
- The slip surfaces investigated can be forced to pass through a specific point at some depth below the surface of the slope.
- The soil mass above the slip surface can be required to have a minimum weight.
- An artificially high shear strength, typically expressed by a high value of cohesion, can be assigned to a zone of soil near the face of the slope so that shallow slip surfaces are prevented. In doing so, care must be exercised to ensure that slip surfaces are not unduly restricted from exiting in the toe area of the slope.

Ambiguities in slip surface location. In some cases it is possible to have a circle where more than one segment of the circle intersects the slope (Figure 7.5). In such cases there is not just a single soil mass above the slip surface, but rather there are multiple, disassociated soil masses, probably with different factors of safety. To avoid ambiguities in this case, it is necessary to be able to designate that only a particular portion of the slope is to be analyzed.

Recapitulation

- Computer programs can be categorized as design programs and analysis programs. Design programs are useful for design of simple reinforced slopes, while analysis programs generally can handle a much wider range of slope and soil conditions.
- Searches to locate a critical slip surface with a minimum factor of safety should begin with circles.

- Multiple searches with different starting points and different values for the other parameters that affect the search should be performed to ensure that the most critical slip surface is found.
- In some case it is appropriate to restrict the region where a search is conducted; however, care must be taken to ensure that an important slip surface is not overlooked.

VERIFICATION OF ANALYSES

Most slope stability analyses are performed using general-purpose computer programs. The computer programs offer a number of features and may involve tens of thousands, and sometimes millions, of lines of computer code with many possible paths through the logic, depending on the problem being solved. Forester and Morrison (1994) point out the difficulty of checking even simple computer programs with multiple combinations of paths through the software. Consider, for example, a comprehensive computer program for slope stability analysis that contains the features listed in Table 7.1. Most of the more sophisticated computer programs probably contain at least the number of options or features listed in this table. Although some programs will not contain all of the options listed, they may contain others. A total of 40 different features and options is listed in Table 7.1. If we consider just two different possibilities for the input values for each option or feature, there will be a total of over 1×10^{12} ($= 2^{40}$) possible combinations and paths through the software. If we could create, run, and verify problems to test each possible combination at the rate of one test problem every 10 minutes, over 20 million years would be required to test all possible combinations, working 24 hours a day, 7 days a week. Clearly, it is not possible to test sophisticated computer programs for all possible combinations of data, or even a reasonably small fraction, say 1 of 1000, of the possible combinations. Consequently, there is a significant possibility that any computer program being used has not been tested for the precise combination of paths involved in a particular problem.

Because it is very possible that any computer program has not been verified for the particular combination of conditions the program is being used for, some form of independent check should be made of the results. This is also true for other methods of calculation. For example, spreadsheets are just another form of computer program, and the difficulty of verifying spreadsheet programs was discussed earlier. It is also possible to make errors in using slope stability charts and even in using simple equations. Furthermore, the simple equations generally are based on approximations that can lead to important errors for some applications. Consequently, regardless of how slope stability computations are performed, some independent check should be made of the results. A number of examples of slope stability analyses and checks that can be made are presented in the next section.

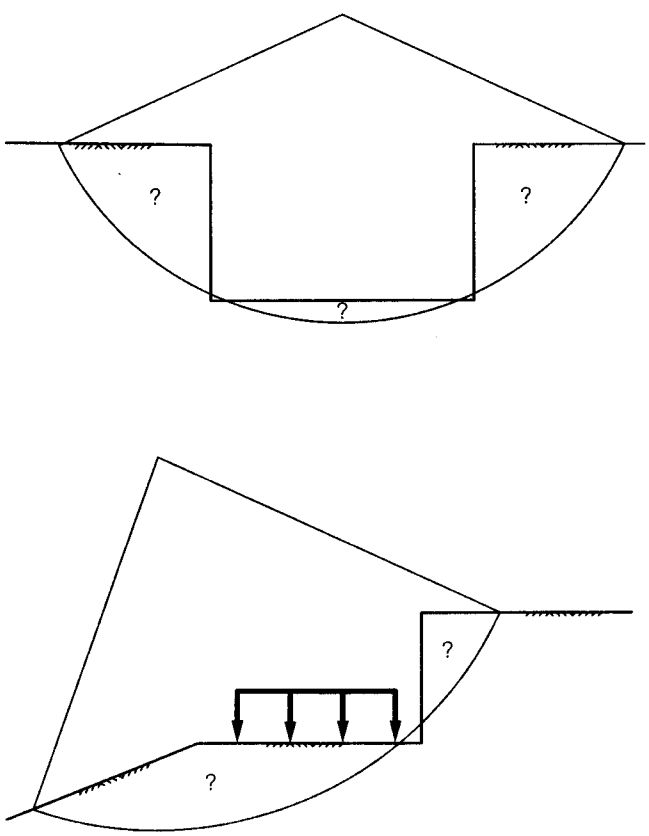

Figure 7.5 Cases where the slide mass defined by a circular slip surface is ambiguous and may require selective restriction.

Recapitulation

- Because of the large number of possible paths through most computer programs, it is likely most programs have not been tested for the precise combination of paths involved in any particular analysis.
- Some check should be made of the results of slope stability calculations, regardless of how the calculations are performed.

CHAPTER 13

Factors of Safety and Reliability

Factors of safety provide a quantitative indication of slope stability. A value of $F = 1.0$ indicates that a slope is on the boundary between stability and instability; the factors tending to make the slope stable are in precise balance with those tending to make the slope unstable. A calculated value of F less than 1.0 indicates that a slope would be unstable under the conditions contemplated, and a value of F greater than 1.0 indicates that a slope would be stable.

If we could compute factors of safety with absolute precision, a value of $F = 1.1$ or even 1.01 would be acceptable. However, because the quantities involved in computing factors of safety are always uncertain to some degree, computed values of F are never absolutely precise. We need larger factors of safety to be sure (or sure enough) that a slope will be stable. How large the factor of safety should be is determined by experience, by the degree of uncertainty that we think is involved in calculating F, and by the consequences that would ensue if the slope failed.

The reliability of a slope (R) is an alternative measure of stability that considers explicitly the uncertainties involved in stability analyses. The reliability of a slope is the computed probability that a slope will not fail and is 1.0 minus the probability of failure:

$$R = 1 - P_f \tag{13.1}$$

where P_f is the probability of failure and R is the reliability or probability of no failure. A method for computing P_f is described later in the chapter. Factors of safety are more widely used than R or P_f to characterize slope stability. Although R and P_f are equally logical measures of stability, there is less experience with their use, and therefore less guidance regarding acceptable values.

Another consideration regarding use of reliability and probability of failure is that it is sometimes easier to explain the concepts of reliability or probability of failure to laypeople. However, some find it disturbing that a slope has a probability of failure that is not zero, and may not be comfortable hearing that there is some chance that a slope might fail. Factors of safety and reliability complement each other, and each has its own advantages and disadvantages. Knowing the values of both is more useful than knowing either one by itself.

DEFINITIONS OF FACTOR OF SAFETY

The most widely used and most generally useful definition of factor of safety for slope stability is

$$F = \frac{\text{shear strength of the soil}}{\text{shear stress required for equilibrium}} \tag{13.2}$$

Uncertainty about shear strength is often the largest uncertainty involved in slope stability analyses, and it is therefore logical that the factor of safety—called by George Sowers the *factor of ignorance*—should be related directly to shear strength. One way of judging whether a value of F provides a sufficient margin of safety is by considering the question: What is the lowest conceivable value of shear strength? A value of $F = 1.5$ for a slope indicates that the slope should be stable even if the shear strength was 33% lower than anticipated (if all the other factors were the same as anticipated). When shear strength is represented in terms of c and ϕ, or c' and ϕ', the same value of F is applied to both of these components of shear strength.

It can be said that this definition of factor of safety is based on the assumption that F is the same for every point along the slip surface. This calls into question

whether such analyses are reasonable, because it can be shown, for example by finite element analyses, that the factor of safety for every slice is *not* the same, and it therefore appears that an underlying assumption of limit equilibrium analysis is not true. However, despite the fact that the local factor of safety may be more or less than the value of F calculated by conventional limit equilibrium methods, the average value calculated by these methods is a valid and very useful measure of stability. The factor of safety determined from conventional limit equilibrium analyses is the answer to the question: By what factor could the shear strength of the soil be reduced before the slope would fail? This is a significant question, and the value of F calculated as described above is the most generally useful measure of stability that has been devised.

Alternative Definitions of F

Other definitions of F have sometimes been used for slope stability. For analyses using circular slip surfaces, the factor of safety is sometimes defined as the ratio of resisting moment divided by overturning moment. Because the resisting moment is proportional to shear strength, and the shear stress required for equilibrium of a mass bounded by a circular slip surface is proportional to the overturning moment, the factor of safety defined as the ratio of resisting to overturning moment is the same as the factor of safety defined by Eq. (13.1).

In times past, different factors of safety were sometimes applied to cohesion and friction. However, this is seldom done any more. The strength parameters c and ϕ, or c' and ϕ', are empirical coefficients in equations that relate shear strength to normal stress or to effective normal stress. There is no clear reason to factor them differently, and the greater complexity that results if this is done seems not to be justified by additional insight or improved basis for judging the adequacy of stability.

Reinforcing and anchoring elements within a slope impose stabilizing forces that, like the soil strength, should be factored to include a margin of safety to reflect the fact that there is uncertainty in their magnitudes. The issues causing uncertainties in reinforcing and anchoring forces are not the same as the issues leading to uncertainties in soil strength, and it is therefore logical to apply different factors of safety to reinforcement and soil strength. This can be achieved by prefactoring reinforcement and anchor forces and including them in stability analyses as known forces that are not factored further in the course of the analysis.

FACTOR OF SAFETY CRITERIA

Importance of Uncertainties and Consequences of Failure

The value of the factor of safety used in any given case should be commensurate with the uncertainties involved in its calculation and the consequences that would ensue from failure. The greater the degree of uncertainty about the shear strength and other conditions, and the greater the consequences of failure, the larger should be the required factor of safety. Table 13.1 shows values of F based on this concept.

Corps of Engineers' Criteria for Factors of Safety

The values of factor of safety listed in Table 13.2 are from the U.S. Army Corps of Engineers' slope stability manual. They are intended for application to slopes of embankment dams, other embankments, excavations, and natural slopes where conditions are well understood and where the properties of the soils have been studied thoroughly. They represent conventional, prudent practice for these types of slopes and conditions, where the consequences of failure may be significant, as they nearly always are for dams.

Recommended values of factor of safety, like those in Table 13.2, are based on experience, which is logical. It is not logical, however, to apply the same values of factor of safety to conditions that involve widely varying degrees of uncertainty. It is therefore significant that the factors of safety in Table 13.2 are intended for Corps of Engineers' projects, where methods of exploration, testing, and analysis are consistent from one project to another and the degree of uncertainty regarding these factors does not vary widely. For other situations, where practices and circumstances differ, the values of F in Table 13.2 may not be appropriate.

RELIABILITY AND PROBABILITY OF FAILURE

Reliability calculations provide a means of evaluating the combined effects of uncertainties and a means of distinguishing between conditions where uncertainties are particularly high or low. Despite the fact that it has potential value, reliability theory has not been used much in routine geotechnical practice because it involves terms and concepts that are not familiar to many geotechnical engineers, and because it is commonly perceived that using reliability theory would require more data, time, and effort than are available in most circumstances.

Table 13.1 Recommended Minimum Values of Factor of Safety

Cost and consequences of slope failure	Uncertainty of analysis conditions	
	Small[a]	Large[b]
Cost of repair comparable to incremental cost to construct more conservatively designed slope	1.25	1.5
Cost of repair much greater than incremental cost to construct more conservatively designed slope	1.5	2.0 or greater

[a]The uncertainty regarding analysis conditions is smallest when the geologic setting is well understood, the soil conditions are uniform, and thorough investigations provide a consistent, complete, and logical picture of conditions at the site.

[b]The uncertainty regarding analysis conditions is largest when the geologic setting is complex and poorly understood, soil conditions vary sharply from one location to another, and investigations do not provide a consistent and reliable picture of conditions at the site.

Table 13.2 Factor of Safety Criteria from U.S. Army Corps of Engineers' Slope Stability Manual

Types of slopes	Required factors of safety[a]		
	For end of construction[b]	For long-term steady seepage	For rapid drawdown[c]
Slopes of dams, levees, and dikes, and other embankment and excavation slopes[c]	1.3	1.5	1.0–1.2

[a]For slopes where either sliding or large deformations have occurred, and back analyses have been performed to establish design shear strengths, lower factors of safety may be used. In such cases probabilistic analyses may be useful in supporting the use of lower factors of safety for design. Lower factors of safety may also be justified when the consequences of failure are small.

[b]Temporary excavated slopes are sometimes designed only for short-term stability, with knowledge that long-term stability would be inadequate. Special care, and possibly higher factors of safety, should be used in such cases.

[c]$F = 1.0$ applies to drawdown from maximum surcharge pool, for conditions where these water levels are unlikely to persist for long enough to establish steady seepage. $F = 1.2$ applies to maximum storage pool level, likely to persist for long periods prior to drawdown. For slopes in pumped storage projects, where rapid drawdown is a normal operating condition, higher factors of safety (e.g., 1.3 to 1.4) should be used.

Harr (1987) defines the engineering definition of *reliability* as follows: "Reliability is the probability of an object (item or system) performing its required function adequately for a specified period of time under stated conditions." As it applies in the present context, the *reliability of a slope* can be defined as follows: The reliability of a slope is the probability that the slope will remain stable under specified design conditions. The design conditions include, for example, the end-of-construction condition, the long-term steady seepage condition, rapid drawdown, and earthquake of a specified magnitude.

The design life of a slope and the time over which it is expected to remain stable are usually not stated explicitly but are generally thought of as a long time, probably beyond the lifetime of anyone alive today. The element of time may be considered more explicitly when design conditions involve earthquakes with a specified return period, or other loads whose occurrence can be stated in probabilistic terms.

Christian et al. (1994), Tang et al. (1999), Duncan (2000), and others have described examples of the use of reliability for slope stability. Reliability analysis can be applied in simple ways, without more data, time, or

effort than are commonly available. Working with the same quantity and types of data, and the same types of engineering judgments that are used in conventional analyses, it is possible to make approximate but useful evaluations of probability of failure and reliability.

The results of simple reliability analyses are neither more accurate nor less accurate than factors of safety calculated using the same types of data, judgments, and approximations. Although neither deterministic nor reliability analyses are precise, they both have value, and each enhances the value of the other. The simple types of reliability analyses described in this chapter require only modest extra effort compared to that required to calculate factors of safety, but they can add considerable value to the results of slope stability analyses.

STANDARD DEVIATIONS AND COEFFICIENTS OF VARIATION

If several tests are performed to measure a soil property, it will usually be found that there is scatter in the values measured. For example, consider the undrained strengths of San Francisco Bay mud measured at a site on Hamilton Air Force Base in Marin County, California, that are shown in Table 13.3. There is no discernible systematic variation in the measured values of shear strength between 10 and 20 ft depth at the site. The differences among the values in Table 13.3 are due to natural variations in the strength of the Bay mud in situ, and varying amounts of disturbance of the test specimens. Standard deviation is a quantitative measure of the scatter of a variable. The greater the scatter, the larger the standard deviation.

Statistical Estimates

If a sufficient number of measurements have been made, the standard deviation can be computed using the formula

$$\sigma = \sqrt{\frac{1}{N-1}\sum_{1}^{N}(x - x_{av})^2} \qquad (13.3)$$

where σ is the standard deviation, N the number of measurements, x the measured variable, and x_{av} the average value of x. Standard deviation has the same units as the measured variable.

The average of the 20 measured values of s_u in Table 13.3 is 0.22 tsf (tons/ft^2). The standard deviation, computed using Eq. (13.3), is

Table 13.3 Undrained Shear Strength Values for San Francisco Bay Mud at Hamilton Air Force Base in Marin County, California[a]

Depth (ft)	Test	s_u (tons/ft^2)
10.5	UU	0.25
	UC	0.22
11.5	UU	0.23
	UC	0.25
14.0	UU	0.20
	UC	0.22
14.5	UU	0.15
	UC	0.18
16.0	UU	0.19
	UC	0.20
	UU	0.23
	UC	0.25
16.5	UU	0.15
	UC	0.18
17.0	UU	0.23
	UC	0.26
17.5	UU	0.24
	UC	0.25
19.5	UU	0.24
	UC	0.21

[a]Values measured in unconfined compression (UC) and unconsolidated–undrained (UU) triaxial compression tests.

$$\sigma_{s_u} = \sqrt{\frac{1}{19}\sum_{1}^{20}(s_u - s_{u,av})^2} = 0.033 \text{ tsf} \qquad (13.4)$$

where s_u is the undrained shear strength and $s_{u,av}$ is the average undrained shear strength = 0.22 tsf. The *coefficient of variation* is the standard deviation divided by the expected value of a variable, which for practical purposes can be taken as the average:

$$\text{COV} = \frac{\sigma}{\text{average value}} \qquad (13.5)$$

where COV is the coefficient of variation, usually expressed in percent. Thus the coefficient of variation of the measured strengths in Table 13.3 is

$$\text{COV}_{s_u} = \frac{0.033}{0.22} = 15\% \qquad (13.6)$$

where COV_{s_u} is the coefficient of variation of the undrained strength data in Table 13.3.

The coefficient of variation is a very convenient measure of scatter in data, or uncertainty in the value of the variable, because it is dimensionless. If all of the strength values in Table 13.3 were twice as large as those shown, the standard deviation of the values would be twice as large, but the coefficient of variation would be the same. The tests summarized in Table 13.3 were performed on high-quality test specimens using carefully controlled procedures, and the Bay mud at the Hamilton site is very uniform. The value of $COV_{s_u} = 15\%$ for these data is about as small as could ever be expected. Harr (1987) suggests that a representative value of $COV_{s_u} = 40\%$.

Estimates Based on Published Values

Frequently in geotechnical engineering, the values of soil properties are estimated based on correlations or on meager data plus judgment, and it is not possible to calculate values of standard deviation or coefficient of variation as shown above. Because standard deviations or coefficients of variation are needed for reliability analyses, it is essential that their values can be estimated using experience and judgment. Values of COV for various soil properties and in situ tests are shown in Table 13.4. These values may be of some use in estimating COVs for reliability analysis, but the values cover wide ranges, and it is not possible to use this type of information to make refined estimates of COV for specific cases.

The 3σ Rule

This rule of thumb, described by Dai and Wang (1992), uses the fact that 99.73% of all values of a normally distributed parameter fall within three standard deviations of the average. Therefore, if HCV is the highest conceivable value of the parameter and LCV is the lowest conceivable value of the parameter, these are approximately three standard deviations above and below the average value.

The 3σ rule can be used to estimate a value of standard deviation by first estimating the highest and lowest conceivable values of the parameter, and then dividing the difference between them by 6:

$$\sigma = \frac{\text{HCV} - \text{LCV}}{6} \tag{13.7}$$

where HCV is the highest conceivable value of the parameter and LCV is the lowest conceivable value of the parameter.

Consider, for example, how the 3σ rule can be used to estimate a coefficient of variation for a friction angle for sand that is estimated based on a correlation with standard penetration test blow count: For a value of $N_{60} = 20$, the *most likely value* (MLV) of ϕ' might be estimated to be 35°. However, no correlation is precise, and the value of ϕ' for a particular sand with an SPT blow count of 20 might be higher or lower than 35°. Suppose that the HCV was estimated to be 45°, and the LCV was estimated to be 25°. Then, using Eq. (13.7), the COV would be estimated to be

$$\sigma'_\phi = \frac{45° - 25°}{6} = 3.3° \tag{13.8}$$

and the coefficient of variation = 3.3°/35° = 9%.

Studies have shown that there is a tendency to estimate a range of values between HCV and LCV that is too small. One such study, described by Folayan et al. (1970), involved asking a number of geotechnical engineers to estimate the possible range of values of $C_c/(1 + e)$ for San Francisco Bay mud, with which

Table 13.4 Coefficients of Variation for Geotechnical Properties and In Situ Tests

Property or in situ test	COV (%)	References
Unit weight (γ)	3–7	Harr (1987), Kulhawy (1992)
Buoyant unit weight (γb)	0–10	Lacasse and Nadim (1997), Duncan (2000)
Effective stress friction angle (ϕ')	2–13	Harr (1987), Kulhawy (1992), Duncan (2000)
Undrained shear strength (S_u)	13–40	Kulhawy (1992), Harr (1987), Lacasse and Nadim (1997)
Undrained strength ratio (s_u/σ'_v)	5–15	Lacasse and Nadim (1997), Duncan (2000)
Standard penetration test blow count (N)	15–45	Harr (1987), Kulhawy (1992)
Electric cone penetration test (q_c)	5–15	Kulhawy (1992)
Mechanical cone penetration test (q_c)	15–37	Harr (1987), Kulhawy (1992)
Dilatometer test tip resistance (q_{DMT})	5–15	Kulhawy (1992)
Vane shear test undrained strength (S_v)	10–20	Kulhawy (1992)

they all had experience. The data collected in this exercise are summarized below:

Average value of $\frac{C_c}{1+e}$ estimate by experienced engineers = 0.29

Average value of $\frac{C_c}{1+e}$ from 45 laboratory tests = 0.34

Average COV of $\frac{C_c}{1+e}$ estimate by experienced engineers = 8%

Average COV of $\frac{C_c}{1+e}$ from 45 laboratory tests = 18%

The experienced engineers were able to estimate the value of $C_c/(1 + e)$ for Bay mud within about 15%, but they underestimated the COV of $C_c/(1 + e)$ by about 55%.

Christian and Baecher (2001) showed that people (experienced engineers included) tend to be overconfident about their ability to estimate values, and therefore estimate possible ranges of values that are narrower than the actual range. If the range between the highest conceivable value (HCV) and the lowest conceivable value (LCV) is too small, values of coefficient of variation estimated using the 3σ rule will also be too small, introducing an unconservative bias in reliability analysis.

Based on statistical analysis, Christian and Baecher (2001) showed that the expected range of values in a sample containing 20 values is 3.7 times the standard deviation, and the expected range of values in a sample of 30 is 4.1 times the standard deviation. This information can be used to improve the accuracy of estimated values of standard deviation by modifying the 3σ rule. If the experience of the person making the estimate encompasses sample sizes in the range of 20 to 30 values, a better estimate of standard deviation would be made by dividing the range between HCV and LCV by 4 rather than 6:

$$\sigma = \frac{\text{HCV} - \text{LCV}}{4} \tag{13.9}$$

If Eq. (13.9) is used to estimate the coefficient of variation of ϕ', the value is

$$\sigma = \frac{45° - 25°}{4} = 5° \tag{13.10}$$

and the coefficient of variation is 5°/35° = 14%.

With the 3σ rule it is possible to estimate values of standard deviation using the same amounts and types of data that are used for conventional deterministic geotechnical analyses. The 3σ rule can be applied when only limited data are available and when no data are available. It can also be used to judge the reasonableness of values of the coefficient of the variation from published sources, considering that the lowest conceivable value would be two or three standard deviations below the mean, and the highest conceivable value would be two or three standard deviations above the mean. If these values seem unreasonable, some adjustment of values is called for.

The 3σ rule uses the simple normal distribution as a basis for estimating that a range of three standard deviations covers virtually the entire population. However, the same is true of other distributions (Harr, 1987), and the 3σ rule is not tied rigidly to any particular probability distribution.

Graphical 3σ Rule

The concept behind the 3σ rule of Dai and Wang (1992) can be extended to a graphical procedure that is applicable to many situations in geotechnical engineering, where the parameter of interest, such as undrained shear strength, varies with depth. An examples is shown in Figure 13.1.

The steps involved in applying the graphical 3σ rule are as follows:

1. Draw a straight line or a curve through the data that represent the most likely average variation of the parameter with depth.
2. Draw straight lines or curves that represent the highest and lowest conceivable bounds on the data. These should be wide enough to include all valid data and an allowance for the fact that the natural tendency is to estimate such bounds too narrowly, as discussed previously. Note that some points in Figure 13.1 are outside the estimated highest and lowest conceivable lines, indicating that these data points are believed to be erroneous.
3. Draw straight lines or curves that represent the average plus one standard deviation and the average minus one standard deviation. These are one-third of the distance (or one-half of the distance) from the average line to the highest and lowest conceivable bounds.

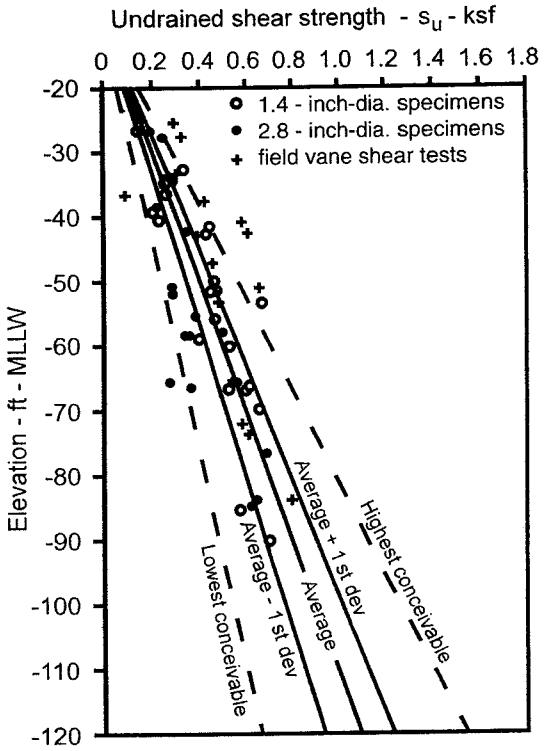

Figure 13.1 Example of graphical 3σ rule for undrained strength profile.

The average-plus-1σ and average-minus-1σ curves or lines are used in the Taylor series method described below in the same way as are parameters that can be represented by single values.

The graphical 3σ rule is also useful for characterizing strength envelopes for soils. In this case the quantity (shear strength) varies with normal stress rather than depth, but the procedure is the same. Strength envelopes are drawn that represent the average and the highest and lowest conceivable bounds on the data, as shown in Figure 13.2. Then average-plus-1σ and average-minus-1σ envelopes are drawn one-third of the distance (or one-half of the distance) from the average envelope to the highest and lowest conceivable bounds.

Using the graphical 3σ rule to establish average-plus-1σ and average-minus-1σ strength envelopes is preferable to using separate standard deviations for the strength parameters c and ϕ. Strength parameters (c and ϕ) are useful empirical coefficients that characterize the variation of shear strength with normal stress, but they are not of fundamental significance or interest by themselves. The important parameter is shear strength, and the graphical 3σ rule provides a straightforward means for characterizing the uncertainty in shear strength.

COEFFICIENT OF VARIATION OF FACTOR OF SAFETY

Reliability and probability of failure can be determined easily once the factor of safety and the coefficient of variation of the factor of safety (COV_F) have been determined. The value of factor of safety is determined in the usual way, using a computer program, slope stability charts, or spreadsheet calculations. The value of COV_F can be evaluated using the Taylor series method, which involves these steps:

1. Estimate the standard deviations of the quantities involved in analyzing the stability of the slope: for example, the shear strengths of the soils, the unit weights of the soils, the piezometric levels, the water level outside the slope, and the loads on the slope.
2. Use the Taylor series numerical method (Wolff, 1994; U.S. Army Corps of Engineers, 1998) to estimate the standard deviation and the coefficient of variation of the factor of safety, using these formulas:

$$\sigma_F = \sqrt{\left(\frac{\Delta F_1}{2}\right)^2 + \left(\frac{\Delta F_2}{2}\right)^2 + \cdots + \left(\frac{\Delta F_N}{2}\right)^2} \tag{13.11}$$

$$\text{COV}_F = \frac{\sigma_F}{F_{\text{MLV}}} \tag{13.12}$$

where $\Delta F_1 = (F_1^+ - F_1^-)$. F_1^+ is the factor of safety calculated with the value of the first parameter increased by one standard deviation from its most likely value, and F_1^- is the factor of safety calculated with the value of the first parameter decreased by one standard deviation.

In calculating F_1^+ and F_1^-, the values of all of the other variables are kept at their most likely values. The other values of ΔF_2, ΔF_3, . . . Δ, F_N are calculated by varying the values of the other variables by plus and minus one standard deviation from their most likely values. F_{MLV} in Eq. (13.12) is the most likely value of factor of safety, computed using most likely values for all the parameters.

Substituting the values of ΔF into Eq. (13.11), the value of the standard deviation of the factor of safety (σ_F) is computed, and the coefficient of variation of the factor of safety (COV_F) is computed using Eq. (13.12). With both F_{MLV} and COV_F known, the probability of failure (P_f) can be determined using Table

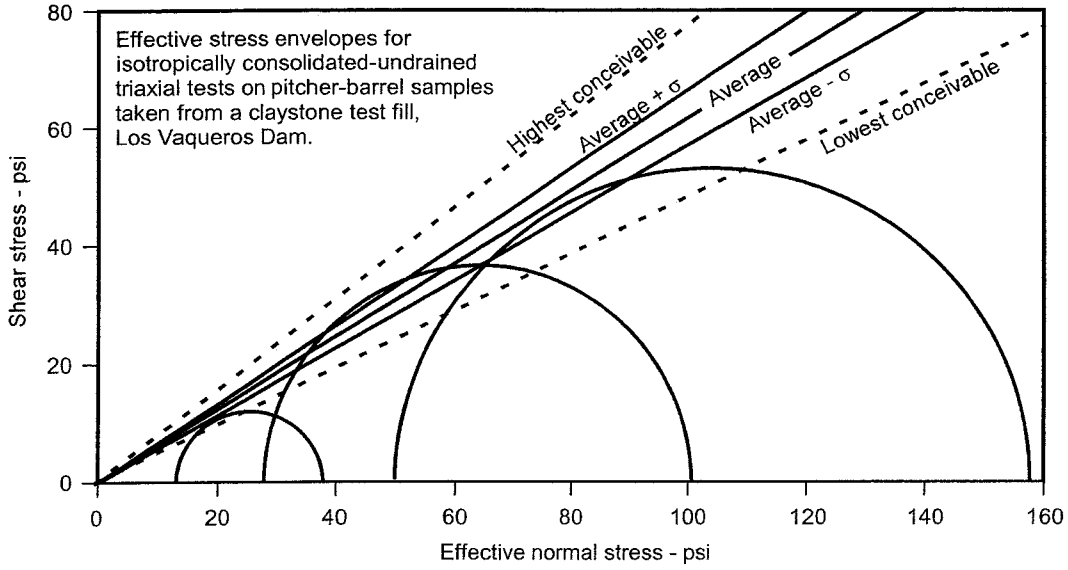

Figure 13.2 Example of graphical 3σ rule for shear strength envelope.

13.5, Figure 13.3, or the reliability index, as explained below.

Table 13.5 and Figure 13.3 assume that the factor of safety is lognormally distributed, which seems reasonable because calculating the factor of safety involves many multiplication and division operations. The central limit theorem indicates that the result of adding and subtracting many random variables approaches a normal distribution as the number of operations increases. Since multiplying and dividing amounts to adding and subtracting logarithms, it follows that the factor of safety distribution can be approximated by a lognormal distribution. Thus, although there is no proof that factors of safety are lognormally distributed, it is at least a reasonable approximation. The assumption of a lognormal distribution for factor of safety does not imply that the values of the individual variables must be distributed lognormally. It is not necessary to make any particular assumption concerning the distributions of the variables to use this method.

RELIABILITY INDEX

The *reliability index* (β) is an alternative measure of safety, or reliability, which is uniquely related to the probability of failure. The value of β indicates the number of standard deviations between $F = 1.0$ (failure) and F_{MLV}, as shown in Figure 13.4. The usefulness of β lies in the fact that probability of failure and reliability are uniquely related to β, as shown in Figure 13.5. The *lognormal reliability index*, β_{LN}, can be determined from the values of F_{MLV} and COV_F using Eq. (13.13):

$$\beta_{LN} = \frac{\ln (F_{MLV}/\sqrt{1 + COV_F^2})}{\sqrt{\ln(1 + COV_F^2)}} \qquad (13.13)$$

where β_{LN} is the lognormal reliability index, F_{MLV} the most likely value of factor of safety, and COV_F the coefficient of variation of factor of safety.

The relationship between β and P_f shown in Figure 13.5 is called the *standard cumulative normal distribution function,* which can be found in many textbooks on probability and reliability. Values of P_f corresponding to a given value of β can be calculated using the NORMSDIST function in Excel. The argument of this function is the reliability index, β_{LN}. In Excel, under "Insert Function," "Statistical," choose "NORMSDIST" and type the value of β_{LN}. The result is the reliability, R. For example, for $\beta_{LN} = 2.32$, the result is 0.9898, which corresponds to $P_f = 0.0102$. Table 13.5 and Figures 13.3 and 13.5 were developed using this Excel function.

PROBABILITY OF FAILURE

Once the most likely value of factor of safety (F_{MLV}) and the coefficient of variation of factor of safety (COV_F) have been evaluated, the probability of failure (P_f) can be determined in any of the following ways:

Table 13.5 Probabilities of Failure (%) Based on Lognormal Distribution of F

	COV_F = coefficient of variation of factor of safety								
F_{MLV}[a]	10%	12%	14%	16%	20%	25%	30%	40%	50%
1.05	33.02	36.38	38.95	41.01	44.14	47.01	49.23	52.63	55.29
1.10	18.26	23.05	26.95	30.15	35.11	39.59	42.94	47.82	51.37
1.15	8.83	13.37	17.53	21.20	27.20	32.83	37.10	43.24	47.62
1.20	3.77	7.15	10.77	14.29	20.57	26.85	31.76	38.95	44.05
1.25	1.44	3.54	6.28	9.27	15.20	21.68	26.98	34.95	40.66
1.30	0.49	1.64	3.49	5.81	11.01	17.30	22.75	31.26	37.48
1.35	0.15	0.71	1.86	3.53	7.83	13.66	19.06	27.88	34.49
1.40	0.04	0.29	0.95	2.08	5.48	10.69	15.88	24.80	31.70
1.50	0.00	0.04	0.23	0.67	2.57	6.38	10.85	19.49	26.69
1.60	0.00	0.01	0.05	0.20	1.15	3.71	7.29	15.21	22.40
1.70	0.00	0.00	0.01	0.06	0.49	2.11	4.84	11.81	18.75
1.80	0.00	0.00	0.00	0.01	0.21	1.18	3.18	9.13	15.67
1.90	0.00	0.00	0.00	0.00	0.08	0.65	2.07	7.03	13.08
2.00	0.00	0.00	0.00	0.00	0.03	0.36	1.34	5.41	10.91
2.20	0.00	0.00	0.00	0.00	0.01	0.10	0.56	3.19	7.59
2.40	0.00	0.00	0.00	0.00	0.00	0.03	0.23	1.88	5.29
2.60	0.00	0.00	0.00	0.00	0.00	0.01	0.09	1.11	3.70
2.80	0.00	0.00	0.00	0.00	0.00	0.00	0.04	0.66	2.60
3.00	0.00	0.00	0.00	0.00	0.00	0.00	0.02	0.39	1.83

[a] F_{MLV}, factor of safety computed using most likely values of parameters.

1. Using Table 13.5
2. Using Figure 13.3
3. Using Figure 13.5, with β_{LN} computed using Eq. (13.13)
4. Using the Excel function NORMSDIST, with β_{LN} computed using Eq. (13.13)

Interpretation of Probability of Failure

The event whose probability is described as the *probability of failure* is not necessarily a catastrophic failure. In the case of shallow sloughing of a slope, for example, failure very likely would not be catastrophic. If the slope could be repaired easily and there were no serious secondary consequences, shallow sloughing would not be catastrophic. However, a slope failure that would be very expensive to repair, or that would have the potential for delaying an important project, or that would involve threat to life, would be catastrophic. Although the term *probability of failure* would be used in both of these cases, it is important to recognize the different nature of the consequences.

In recognition of this important distinction between catastrophic failure and less significant performance problems, the Corps of Engineers uses the term *probability of unsatisfactory performance* (U.S. Army Corps of Engineers, 1998). Whatever terminology is used, it is important to keep in mind the real consequences of the event analyzed and not to be blinded by the word *failure* where the term *probability of failure* is used.

Probability of Failure Criteria

There is no universally appropriate value of probability of failure. Experience indicates that slopes designed in accord with conventional practice often have a probability of failure in the neighborhood of 1%, but like factor of safety, the appropriate value of P_f should depend on the consequences of failure.

One important advantage of probability of failure is the possibility of judging an acceptable level of risk based on the potential cost of failure. Suppose, for example, that two alternative designs for the slopes on a project are analyzed, with these results:

- *Case A.* Steep slopes, construction and land costs = \$100,000, $P_f = 0.1$.
- *Case B.* Flat slopes, construction and land costs = \$400,000, $P_f = 0.01$.

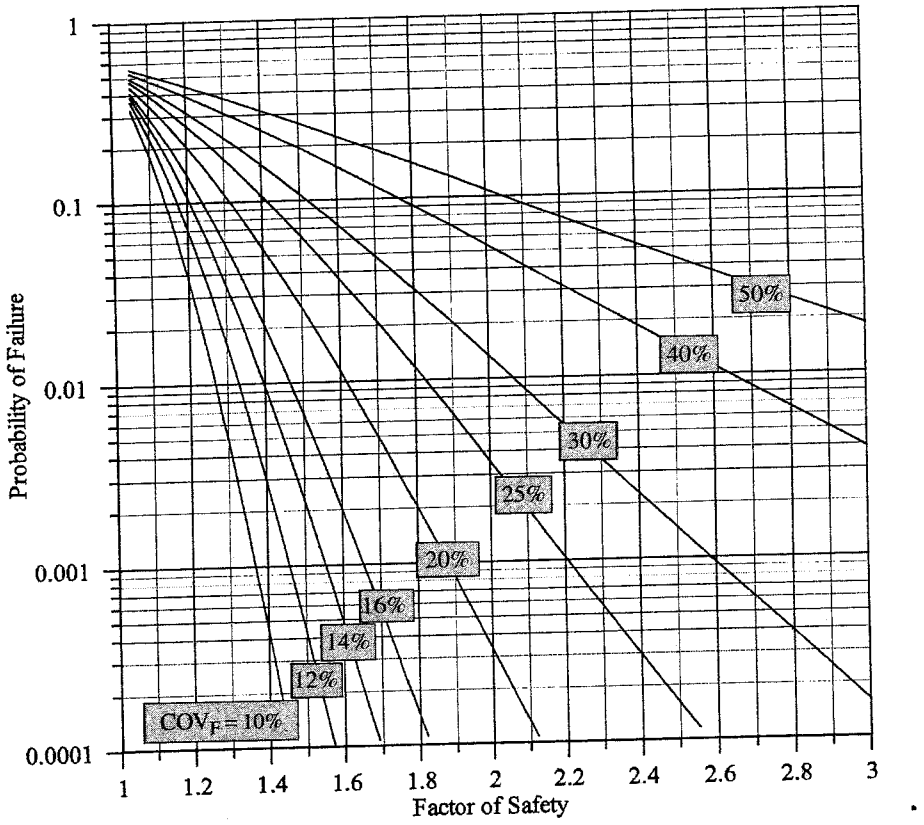

Figure 13.3 Probabilities of failure based on lognormal distribution of F.

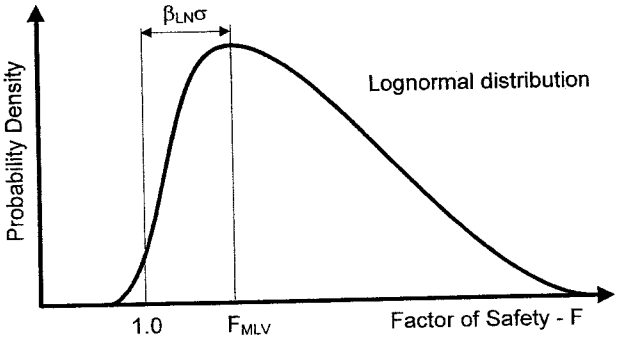

Figure 13.4 Relationship of β_{LN} to probability distribution.

Suppose further that the consequences of failure are estimated to be the same in either case, \$5,000,000, considering primary and secondary consequences of failure. In case A, the total cost of construction, land, and probable cost of failure is \$100,000 + (0.1)(\$5,000,000) = \$600,000. In case B, the total cost is \$400,000 + (0.01)(\$5,000,000) = \$450,000. Considering the probable cost of failure, as well as construction and land costs, case B is less costly overall.

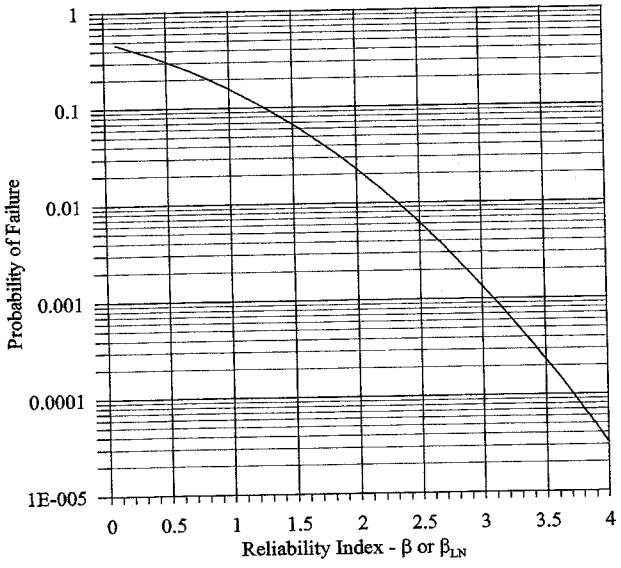

Figure 13.5 Variation of P_f with β.

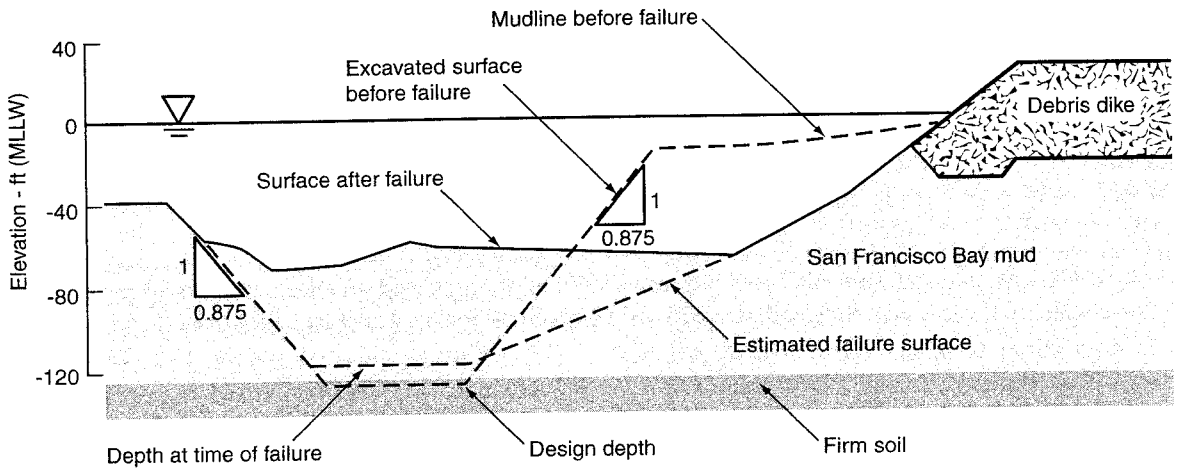

Figure 13.6 Underwater slope failure in San Francisco Bay.

Even without cost analysis, P_f may provide a better basis for judging what is an acceptable risk than does factor of safety. Many people may find that comparing one chance in 10 with one chance in 100 provides a more understandable basis for decision than does comparing a factor of safety of 1.3 with a factor of safety of 1.5.

Example. In August 1970, a trench about 100 ft deep was excavated underwater in San Francisco Bay. The trench was to be filled with sand to stabilize the adjacent area and reduce seismic deformations at a new lighter aboard ship (LASH) terminal. The trench slopes were made steeper than was the normal practice in order to reduce the volume of excavation and fill. As shown in Figure 13.6, the slopes were excavated at an inclination of 0.875 horizontal to 1.0 vertical.

On August 20, after a section of the trench about 500 ft long had been excavated, the dredge operator found that the clamshell bucket could not be lowered to the depth from which mud had been excavated only hours before. Using the side-scanning sonar with which the dredge was equipped, four cross sections made within two hours showed that a failure had occurred that involved a 250-ft-long section of the trench. The cross section is shown in Figure 13.6. Later, a second failure occurred, involving an additional 200 ft of length along the trench. The rest of the 2000-ft-long trench remained stable for about four months, at which time the trench was backfilled with sand. Additional details regarding the failure can be found in Duncan and Buchignani (1973).

Figure 13.1 shows the variation of undrained strength of the Bay mud at the site, and the average, average + σ and average − σ lines established by Duncan (2000) for a reliability analysis of the slope. The average buoyant unit weight of the Bay mud was 38 pcf and the standard deviation was 3.3 pcf, based on measurements made on undisturbed samples.

Factors of safety calculated using average values of strength and unit weight (F_{MLV}) and using average $+\sigma$ and average $-\sigma$ values are shown in Table 13.6. The ΔF value for variation in Bay mud strength is 0.31, and the ΔF value for unit weight variation is 0.20. The ΔF due to strength variation is always significant, but

Table 13.6 Reliability Analysis for 0.875 Horizontal on 1.0 Vertical Underwater Slope in San Francisco Bay Mud

Variable	Values	F	ΔF
Undrained shear strength Buoyant unit weight	Average line in Figure 13.1 $\gamma_{b(av)}$ = 38 pcf	F_{MLV} = 1.17	—
Undrained shear strength	Average + σ line in Figure 13.1	F^+ = 1.33	0.31
	Average − σ line in Figure 13.1	F^- = 1.02	
Buoyant unit weight	Average + σ = 41.3 pcf	F^+ = 1.08	0.20
	Average − σ = 34.7 pcf	F^- = 1.28	

Table 13.7 Summary of Analyses of LASH Terminal Trench Slope

Case	Slope (H on V)	F_{MLV}	COV_F[a] (%)	P_f (%)	Trench volume[b] (yd^3)
As constructed	0.875 on 1.0	1.17	16%	18%	860,000
Less-steep A	1.25 on 1.0	1.3	16%	6%	1,000,000
Less-steep B	1.6 on 1.0	1.5	16%	1%	1,130,000

[a]The value of COV_F is the same for all cases because COVs of strength and unit weight are the same for all cases.
[b]For the as-constructed case, an additional 100,000 yd^3 of slumped material had to be excavated after the failure.

it is unusual for the ΔF due to unit weight variation to be as large as it is in this case. Its magnitude in this case is due to the fact that the buoyant unit weight is so low, only 38 pcf. Therefore, the variation by ± 3.3 pcf has a significant effect.

The standard deviation and coefficient of variation of the factor of safety are calculated using Eqs. (13.11) and (13.12):

$$\sigma_F = \sqrt{\left(\frac{0.31}{2}\right)^2 + \left(\frac{0.20}{2}\right)^2} = 0.18 \quad (13.14)$$

$$COV_F = \frac{0.18}{1.17} = 16\% \quad (13.15)$$

The probability of failure corresponding to these values of F_{MLV} and COV_F can be determined using any of the four methods discussed previously. A value of $P_f = 18\%$ was determined using the Excel function NORMSDIST. Such a large probability of failure is not in keeping with conventional practice. Although it appeared in 1970, when the slope was designed, that the conditions were known well enough to justify using a very low factor of safety of 1.17, the failure showed otherwise. Based on this experience, it is readily apparent that such a low factor of safety and such a high probability of failure exceed the bounds of normal practice. The probability of failure was computed after the failure (Duncan, 2000) and was not available to guide the design in 1970. In retrospect, it seems likely that knowing that the computed probability of failure was 18% might have changed the decision to make the trench slopes so steep.

The cost of excavating the mud that slid into the trench, plus the cost of extra sand backfill, was approximately the same as the savings resulting from the use of steeper slopes. Given the fact that the expected savings were not realized, that the failure caused great alarm among all concerned, and that the confidence of the owner was diminished as a result of the failure, it is now clear that using 0.875 (horizontal) on 1 (vertical) slopes was not a good idea.

Further analyses have been made to determine what the probability of failure would have been if the inboard slope had been excavated less steep. Two additional cases have been analyzed, as summarized in Table 13.7. The analyses were performed using the chart developed by Hunter and Schuster (1968) for shear strength increasing linearly with depth, which is given in the Appendix. The factors of safety for the less-steep alternatives A and B are in keeping with the factor of safety criteria of the Corps of Engineers, summarized in Table 13.2.

A parametric study such as the one summarized in Table 13.7 provides a basis for decision making and for enhanced communication among the members of the design team and with the client. The study could be extended through estimates of the costs of construction for the three cases and estimates of the potential cost of failure. This would provide a basis for the design team and clients to decide how much risk should be accepted. This type of evaluation was not made in 1970 because only factors of safety were computed to guide the design.

Recapitulation

- Uncertainty about shear strength is usually the largest uncertainty involved in slope stability analyses.
- The most widely used and most generally useful definition of factor of safety for slope stability is

$$F = \frac{\text{shear strength of the soil}}{\text{shear stress required for equilibrium}}$$

- The value of the factor of safety used in any given case should be commensurate with the uncertainties involved in its calculation and the consequences of failure.
- Reliability calculations provide a means of evaluating the combined effects of uncertainties and a means of distinguishing between conditions where uncertainties are particularly high or low.

- Standard deviation is a quantitative measure of the scatter of a variable. The greater the scatter, the larger the standard deviation. The coefficient of variation is the standard deviation divided by the expected value of the variable.
- The 3σ rule can be used to estimate a value of standard deviation by first estimating the highest and lowest conceivable values of the parameter and then dividing the difference between them by 6. If the experience of the person making the estimate encompasses sample sizes in the range of 20 to 30 values, a better estimate of standard deviation can be made by dividing by 4 rather than 6.

- Reliability and probability of failure can readily be determined once the factor of safety (F_{MLV}) and the coefficient of variation of the factor of safety (COV_F) have been determined, using the Taylor series numerical method.
- The event whose probability is described as the probability of failure is not necessarily a catastrophic failure. It is important to recognize the nature of the consequences of the event and not to be blinded by the word *failure*.
- The principal advantage of probability of failure, in contrast with factor of safety, is the possibility of judging acceptable level of risk based on the estimated cost and consequences of failure.

Recapitulation

- Convergence criteria that are too coarse can result in false minima and an incorrect location for the critical slip surface.
- Convergence criteria for force and moment imbalance should be scaled to the size of the slope. Tolerances of 100 lb/ft (0.1 kN/m) and 100 ft-lb/ft (0.1 kNm/m) are suitable for most slopes.
- The number of slices does not have a large effect on the computed factor of safety, provided that details of the slope and subsurface stratigraphy are represented.
- For hand calculations only a small number of slices (6 to 12) is required to be consistent with the accuracy achievable by hand calculations.
- For computer solutions with circular slip surfaces, the number of slices is usually chosen by selecting a maximum subtended angle, θ_s, of 3° per slice.
- For computer solutions with noncircular slip surfaces, 30 or more slices are used. Slices are subdivided to produce approximately equal lengths for the base of the slices along the slip surface.

VERIFICATION OF CALCULATIONS

Any set of slope stability calculations should be checked by some independent means. Numerous examples of how analyses can be checked have already been presented in Chapter 7. Also, Duncan (1992) summarized several ways in which the results of slope stability calculations can be checked, including:

1. Experience (what has happened in the past and what is reasonable)
2. By performing extra analyses to confirm the method used by comparison with known results
3. By performing extra analyses to be sure that changes in input causes changes in results that are reasonable
4. By comparing key results with computations performed using another computer program, slope stability charts, spreadsheet, or detailed hand calculations

Many slope stability calculations are performed with a computer program that uses a complete equilibrium procedure of slices. Most of these complete equilibrium procedures (Spencer, Morgenstern and Price, Chen and Morgenstern, etc.) are too complex for calculation by hand. In this case suitable manual checks of the calculations can be made using force equilibrium procedures and assuming that the interslice forces are inclined at the angle(s) obtained from the computer solution. Suitable spreadsheets for this purpose and example calculations are presented in Chapter 7.

Published benchmark problems also provide a useful way for checking the validity of computer codes, and although benchmarks do not verify the solution for the particular problem of interest, they can lend confidence that the computer software is working properly and that the user understands the input data. Several compilations of benchmark problems have been developed and published for this purpose (e.g., Donald and Giam, 1989; Edris and Wright, 1987).

In addition to benchmark problems there are several ways that simple problems can be developed to verify that computer codes are working properly. Most of these simple problems are based on the fact that it is possible to model the same problem in more than one way. Examples of several simple test problems are listed below and illustrated in Figures 14.22 and 14.23:

1. Computation of the factor of safety for a submerged slope under drained conditions using:
   a. Total unit weights, external loads representing the water pressures, and internal pore water pressures
   b. Submerged unit weights with no pore water pressure or external water loads

   This is illustrated in Figure 14.22*a*. Both approaches should give the same factor of safety.[3]
2. Computation of the factor of safety with the same slope facing to the left and to the right (Figure 14.22*b*). The factor of safety should not depend on the direction that the slope faces.
3. Computation of the factor of safety for a partially or fully submerged slope, treating the water as:
   a. An externally applied pressure on the surface of the slope
   b. A "soil" with no strength ($c = 0$, $\phi = 0$) and having the unit weight of water.

   This is illustrated in Figure 14.22*c*.
4. Computation of the factor of safety for a slope with very long internal reinforcement (geogrid, tieback) applying the reinforcement loads as:
   a. External loads on the slope
   b. As internal loads at the slip surface

[3] See also the discussion in Chapter 6 of water pressures and how they are handled. Large differences between the two ways of representing water pressures may occur if force equilibrium procedures are used. See also Example 2 in Chapter 7.

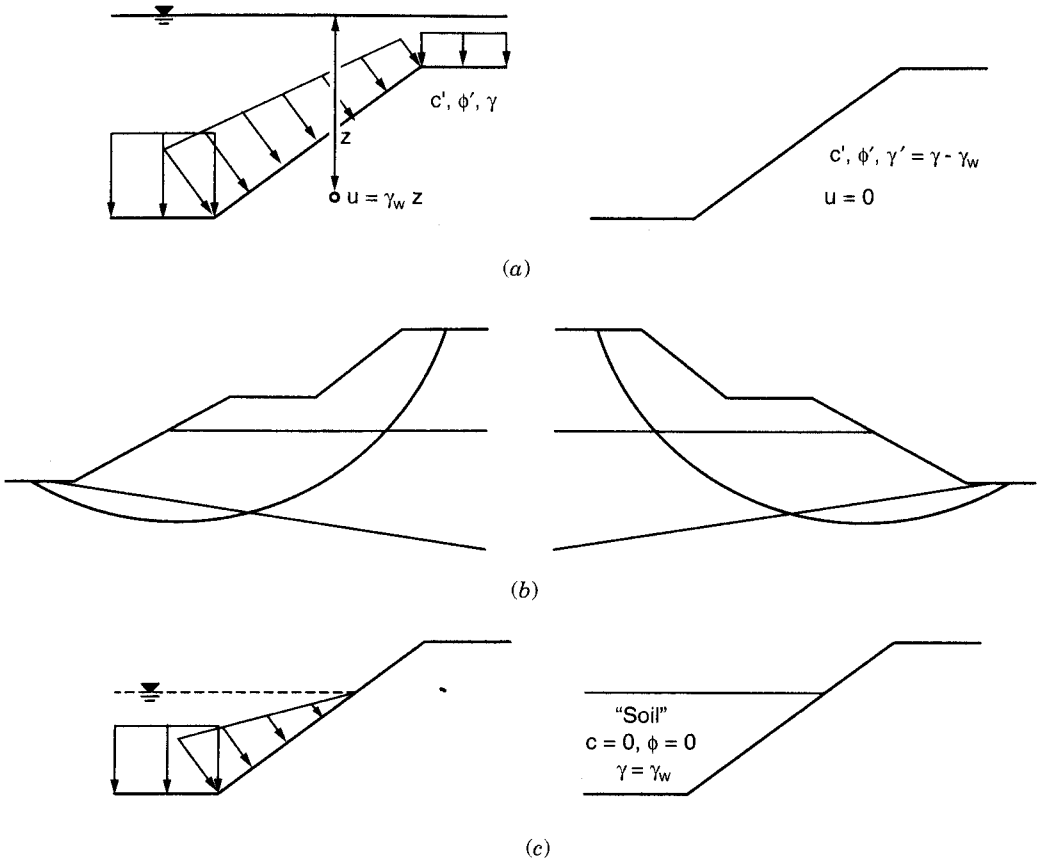

Figure 14.22 Equivalent representations for selected slope problems: (*a*) simple submerged slope, no flow; (*b*) left- and right-facing slope; (*c*) partially submerged slope.

This is illustrated in Figure 14.23*a*. Although intuitively the location where the force is applied might be expected to have an effect, the location does not have a large effect on the computed factor of safety, provided that the slip surface does not pass behind the reinforcement and the force does not vary along the length of the reinforcement.

5. Computation of the bearing capacity of a uniformly loaded strip footing on a horizontal, infinitely deep, purely cohesive foundation (Figure 14.23*b*). For circular slip surfaces and a bearing pressure equal to 5.53 times the shear strength (c) of the soil, a factor of safety of unity should be calculated.
6. Computation of the seismic stability of a slope using:
   a. A seismic coefficient, k
   b. No seismic coefficient, but the slope is steepened by rotating the entire slope geometry through an angle, θ, where the tangent of θ is the seismic coefficient (i.e., $k = \tan\theta$) *and* the unit weight is increased by multiplying the actual unit weight by $\sqrt{1 + k^2}$

   This is illustrated in Figure 14.23*c*. In both solutions the magnitude and direction of the forces will be the same and should produce the same factor of safety.

Additional test problems can also be created using slope stability charts like the ones presented in the Appendix.

THREE-DIMENSIONAL EFFECTS

All the analysis procedures discussed in Chapter 6 assume that the slope is infinitely long in the direction perpendicular to the plane of interest; failure is assumed to occur simultaneously along the entire length of the slope. A two-dimensional (plane strain) cross section is examined, and equilibrium is considered in